

Rethinking Federated Unlearning via the Lens of Memorization

Jiaheng Wei
Royal Melbourne Institute of
Technology
Melbourne, VIC, Australia
wei.jiaheng@rmit.edu.au

Yanjun Zhang
Griffith University
Brisbane, QLD, Australia
yanjun.zhang@griffith.edu.au

He Zhang
Griffith University
Brisbane, QLD, Australia
h.zhang@griffith.edu.au

Leo Yu Zhang
Griffith University
Gold Coast, QLD, Australia
leo.zhang@griffith.edu.au

Chao Chen*
Royal Melbourne Institute of
Technology
Melbourne, VIC, Australia
chao.chen@rmit.edu.au

Kok-Leong Ong
Royal Melbourne Institute of
Technology
Melbourne, VIC, Australia
kok-leong.ong2@rmit.edu.au

Jun Zhang
Swinburne University of Technology
Melbourne, VIC, Australia
junzhang@swin.edu.au

Yang Xiang
Swinburne University of Technology
Melbourne, VIC, Australia
yxiang@swin.edu.au

Abstract

Federated learning (FL) increasingly needs machine unlearning to comply with privacy regulations. However, existing federated unlearning approaches may overlook the overlapping information between the unlearning and remaining data, leading to ineffective unlearning and unfairness between clients. In this work, we revisit federated unlearning through the lens of memorization. We argue that unlearning should mainly remove the unique memorized information attributable to the data to be forgotten, while preserving overlapping patterns that are also supported by the remaining data. Specifically, we propose Grouped Memorization Evaluation, an example-level metric that separates memorized knowledge from overlapping knowledge. Building on this metric, we introduce Federated Memorization Pruning (FedMemPrune), a pruning-based unlearning approach that resets redundant parameters responsible for memorization. Extensive experiments show that FedMemPrune closely matches retraining-based unlearning baselines while more effectively eliminating memorization than existing federated unlearning algorithms, yielding strong unlearning performance without sacrificing the utility of retained knowledge.

CCS Concepts

• **Computing methodologies** → **Machine learning**; • **Security and privacy**;

Keywords

Federated learning, Federated unlearning, Memorization

*Corresponding author.



This work is licensed under a Creative Commons Attribution 4.0 International License. *KDD 2026, Jeju Island, Republic of Korea.*
© 2026 Copyright held by the owner/author(s).
ACM ISBN 979-8-4007-2259-2/2026/08
<https://doi.org/10.1145/3770855.3817785>

ACM Reference Format:

Jiaheng Wei, Yanjun Zhang, He Zhang, Leo Yu Zhang, Chao Chen, Kok-Leong Ong, Jun Zhang, and Yang Xiang. 2026. Rethinking Federated Unlearning via the Lens of Memorization. In *Proceedings of the 32nd ACM SIGKDD Conference on Knowledge Discovery and Data Mining V.2 (KDD 2026), August 9–13, 2026, Jeju Island, Republic of Korea*. ACM, New York, NY, USA, 23 pages. <https://doi.org/10.1145/3770855.3817785>

Resource Availability:

The source code of this paper has been made publicly available at <https://doi.org/10.5281/zenodo.20258278> and <https://github.com/JWei1999/Rethinking-Federated-Unlearning-via-the-Lens-of-Memorization>.

1 Introduction

Federated learning (FL) has become a popular machine learning paradigm in recent years [33]. It enables collaborative model training without sharing raw data, where participants train locally and exchange only model updates. An essential requirement of federated learning is federated unlearning (FU) [22]. This concept is referred to as the right to be forgotten (RTBF) [30], as mandated by privacy regulations such as the General Data Protection Regulation (GDPR) [44] and the California Consumer Privacy Act (CCPA) [17]. Consequently, incorporating unlearning mechanisms into FL is essential to maintain user privacy and meet legal requirements.

A straightforward approach for federated unlearning is to retrain the federated learning model. However, retraining involves significant computational and communication costs. Consequently, performing unlearning directly on the original model is a more efficient way. Several federated unlearning (FU) techniques have been proposed to address this challenge. For example, perturbing information representations can facilitate unlearning. Gu et al. [14] fine-tune the original model using a randomly labeled unlearning dataset to compromise the learned representations. Furthermore, historical information can also support unlearning. FedRecovery [52] employs differential privacy and historical updates to make the unlearning data indistinguishable. Additionally, gradient ascent is another widely adopted strategy. Halimi et al. [16] apply this

technique to reverse the learning process, incorporating a l_2 norm constraint to prevent arbitrary updates. FedOSD [34] modifies the loss function and addresses gradient conflicts during unlearning to retain generalization performance. Besides, the loss function optimization based on the Fisher Information Matrix (FIM) [30] has proven effective in guiding unlearning.

However, existing federated unlearning algorithms may overlook the overlapping learnable information between the unlearning and remaining clients. For example, Pan et al. [34] and Halimi et al. [16] attempt to eliminate the influence of the entire unlearning dataset, including the overlapping information. Such removal or oversight may result in ineffective unlearning and unfairness among clients.

Intuitively, in the unlearning setting, the remaining data and the unlearning data typically share similar and overlapping features, implying that they may provide similar information during standard model training. **This raises a key question: should the overlapping information between the unlearning data and the remaining data be removed during unlearning?** In Figure 1, we show the distribution of real embedding features learned by the original model and retrained model in a federated learning scenario. We observe that, in the retrained model, data points from the unlearning client (light red) still exhibit substantial overlap with those from the remaining clients (light green and blue) and are not unlearned. Only a small subset of data points from the unlearning client (deep red) are misclassified by the retrained model. This observation suggests that the overlapping information provided by the remaining clients preserves knowledge of certain data points from the unlearning client. Moreover, it indicates that overlapping information encodes general and shared knowledge rather than client-specific memorization.

Therefore, we argue that overlapping information should not be unlearned. Our argument is based on three main considerations. **1) Generalization.** As suggested by the observations in Figure 1, removing overlapping information may degrade the model’s overall generalization capability, since such information often captures low-level and broadly transferable knowledge. **2) Fairness.** Unlearning overlapping information may disproportionately affect clients that contribute similar content, thereby introducing unfairness into the unlearning process. For example, in Figure 1, the remaining client no. 0 (light blue) contains more overlapping information than the remaining client no. 1 (light green). As a result, removing overlapping information may lead to a larger performance drop for client no. 0 than for client no. 1. **3) Relearning.** Even when overlapping information is removed, it can often be relearned from the remaining data because it is shared across clients and typically represents common, transferable patterns rather than client-specific knowledge.

To address these challenges, we revisit the federated unlearning problem from a memorization perspective. The overlapping features represent shared and generalized information found in both the unlearning and remaining datasets. In contrast, the non-overlapping features correspond to unique and memorization-related information specific to the unlearning dataset and the remaining dataset, respectively. Based on this insight, we identify that the key difference at the information level between the original model and the retrained model lies in the synergistic information jointly provided by the unlearning dataset and remaining dataset and the memorization

information contained within the unlearning dataset. Furthermore, we analyze that the synergistic information can be neglected in general unlearning scenarios.

In conclusion, federated unlearning should not erase all information contained in the deleted client data. If some information is shared by the remaining clients, removing it would harm utility and exceed the intended forgetting target. Therefore, our goal is to remove client-specific memorized information while preserving overlapping information supported by the remaining clients.

Motivated by this insight, we propose federated memorization unlearning, which demonstrates that removing the unique memorization specific to the unlearning dataset, rather than the entire unlearning dataset, can achieve the similar information level as the retraining baseline. Given the lack of an exact metric for unique or memorization information in unlearning, we introduce a novel evaluation metric based on the memorization score [10], enabling a finer-grained assessment of unlearning effectiveness. In addition, we present a novel federated unlearning method that focuses on eliminating the memorization information of the unlearning data, namely FedMemPrune. We identify redundant parameters as the primary carriers of memorization information, making them key targets for removal in unlearning. Consequently, the overlapping information is preserved in the unlearned model to maintain generalization performance and ensure fairness among clients. Experimental results demonstrate that our approach closely matches the retraining baseline and outperforms existing baselines in terms of unlearning efficacy, generalization performance, and client fairness.

Specifically, our contributions can be summarized as follows:

- We analyze the federated unlearning problem based on information theory and propose federated memorization unlearning. We demonstrate that overlapping or shared information, should not be unlearned.
- We propose **Grouped Memorization Evaluation**, a novel metric that can measure memorization information at example level, thereby enabling a fine-grained assessment of unlearning efficacy.
- We introduce the **Federated Memorization Pruning**, a method designed to selectively remove memorization information during unlearning. This approach preserves shared, overlapping knowledge, thereby maintaining generalization performance and promoting fairness across clients.

2 Related Works

2.1 Machine Unlearning

Machine unlearning (MU) aims to selectively remove the influence of specific training samples from a trained model, making it behave as if those samples were never included [3]. While retraining from scratch guarantees exact removal [47], it is prohibitively expensive for large deep models, motivating more efficient MU methods. According to the taxonomy of machine unlearning [26], approaches fall into exact and approximate unlearning. A notable exact method is SISA [2], which partitions data into shards and retrains only the affected sub-model upon deletion. Approximate unlearning includes gradient-based methods such as negative gradient descent [20], random label perturbation [8], and influence

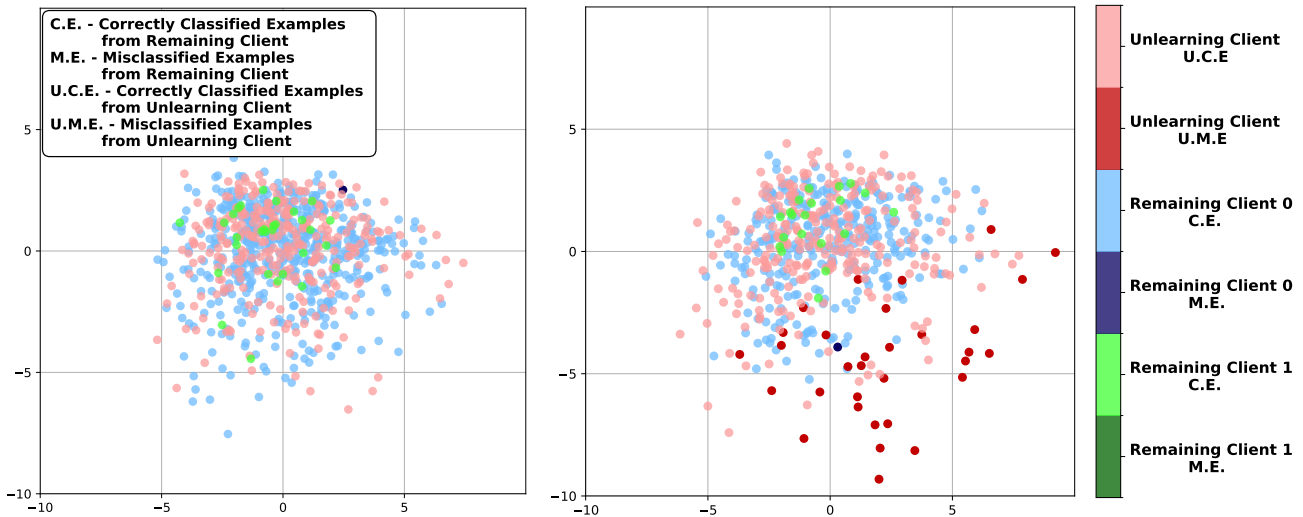


Figure 1: Embedding feature distributions for class-1 on the original model (Left) and the retained model (Right) in FL. In the retained model, some unlearning samples (light red) overlap with remaining-client samples and these points are not fully forgotten.

function-based approaches [12, 15], which leverage the Hessian or Fisher information to revert models toward an unlearned state.

2.2 Memorization Effect

Recent studies [9, 10, 51] reveal that DNNs often memorize specific details instead of learning general patterns, impacting generalization, security, and privacy, and closely relating to unlearning. Feldman [9], Feldman and Zhang [10] propose the memorization score to measure memorization and find the long-tail theory: DNNs tend to memorize atypical examples, because loss optimization drives networks to memorize unique and atypical features, which aid generalization but also increase privacy risks.

Long-tail distributions provide an important lens for understanding memorization. Head classes and common feature patterns are repeatedly reinforced and thus tend to form generalizable representations, while tail samples receive weaker population-level support and may be fitted through instance-specific memorization. This creates a natural connection between long-tail learning and unlearning: when removing some examples, the goal should not be to erase all information contained in these examples since some information may also be supported by remaining examples, but to remove memorized information concentrated in rare or poorly supported regions of the data distribution. This motivates studying memorization-aware unlearning under long-tail distributions and evaluating whether unlearning methods can remove tail information while preserving shared knowledge.

Additional empirical evidence [4, 5] shows that memorization drives privacy vulnerabilities. Maini et al. [32] locate memorization within a small subset of neurons across layers and show that frequent parameter updates mitigate it.

2.3 Federated Unlearning

Federated unlearning (FU) extends machine unlearning to federated learning settings. Following a recent survey [21], existing FU methods can be grouped into 4 main categories. The first category is based on historical information, aiming to revert the model to a pre-learning state. A typical approach is SISA [2], which clusters clients and removes clusters containing the target clients during the unlearning process. Furthermore, historical information can be used to reconstruct an unlearned model. Following this approach, FedEraser [29] enhances model reconstruction efficiency, while FedRecovery [52] improves indistinguishability between unlearned and retained models. Additionally, knowledge distillation can be employed to recover model performance [49]. The second category involves gradient or weight manipulation, which aims to remove or impair learned representations associated with the data through perturbation [7, 8, 14, 53] or pruning techniques [43, 45]. A latest approach [23] proposes NoT, which utilizes weight negation to induce unlearning while preserving model optimality, thereby enabling rapid recovery. The third category focuses on loss function approximation. The unlearning process can be guided using second-order information, such as the Hessian matrix. Liu et al. [30] proposed leveraging the Fisher information matrix as an approximation of the Hessian to optimize the unlearning process. The fourth category involves reversing the training process. A representative method is gradient ascent [16]. Recently, Pan et al. [34] addressed challenges related to gradient exploration and directional conflicts by proposing FedOSD.

Overall, these four technical pathways encompass most existing federated unlearning methods. However, current approaches largely overlook the relationship between unlearning data and remaining data, as well as how this relationship impacts the unlearning process. Additionally, several prior studies [42, 50] highlight that current

unlearning evaluation protocols are insufficient to reliably verify unlearning effectiveness. Thus, federated unlearning requires a fine-grained evaluation framework to rigorously assess its efficacy.

3 Preliminaries

3.1 Federated Learning

Federated learning [24, 33, 38] algorithm f is a distributed learning framework that enables the training of a global model Φ_G by iteratively aggregating knowledge from multiple distributed K clients $C = \{C_k \mid k \in K\}$ without transferring their local datasets $D = \{D_k \mid k \in K\}$. All local datasets D_k are drawn from the data distribution \mathbb{D} . At the core of FL lies an algorithmic process where each client C_k trains a local model Φ_k on its private dataset D_k and periodically communicates the resulting parameters or gradients to a central server. The server then aggregates these updates with specific aggregation algorithms such as Federated Averaging Aggregation [33], to generate the shared global model $\Phi_G \leftarrow f(D)$, which is subsequently redistributed to the clients for further training.

3.2 Federated Unlearning

Federated unlearning is a subfield of machine unlearning that satisfies the requirements of privacy regulations and user rights in the distributed environment. It focuses on deleting the data locally and removing the influence of data from the global model and all local models [31].

DEFINITION 1. Federated Unlearning. We define that $D = \{D_k \mid k \in K\}$ is the set of all local datasets of clients that includes unlearning datasets D_u and remaining datasets D_r . It is worth noting that $D = D_u \cup D_r$. The global model Φ_G is trained on D with federated learning algorithm f that $\Phi_G \leftarrow f(D)$. Thus, the unlearned global model Φ_{G_u} should satisfy:

$$\mathbb{M}_{\Phi_{G_u} \leftarrow A(\Phi_G, D_u)}(\Phi_{G_u}(\mathbb{D})) \approx \mathbb{M}_{\Phi_{G_r} \leftarrow f(D_r)}(\Phi_{G_r}(\mathbb{D})), \quad (1)$$

where A is the federated unlearning algorithm, Φ_{G_u} and Φ_{G_r} are the unlearned global model and the retrained global model respectively, generated by the unlearning process $\Phi_{G_u} \leftarrow A(\Phi_G, D_u)$ and the federated learning retraining $\Phi_{G_r} \leftarrow f(D_r)$. The \mathbb{M} denotes a measurement of the model output distribution, such as accuracy. Moreover, \mathbb{D} is the underlying data distribution that all local dataset D_k are sampled from it. The unlearning dataset D_u , the remaining dataset D_r , and the test dataset D_{test} are sampled from the distribution \mathbb{D} .

Therefore, we conclude that the goal of federated unlearning is to use A to produce an unlearning model Φ_{G_u} that has a similar output distribution to the retrained model Φ_{G_r} on the underlying data distribution \mathbb{D} . Furthermore, federated unlearning may involve different unlearning targets that depend on requests. Generally, the participants in FL can request to unlearn examples, classes and clients. **In this paper, we focus on client unlearning.** Furthermore, the unlearning dataset is defined as $D_u = \{D_k\}_{k \in K_u}$, while the remaining dataset is given by $D_r = \{D_k\}_{k \in K_r}$. Here, K_u and K_r denote the index sets corresponding to the unlearning clients and the remaining clients, respectively.

4 Understanding Memorization in Federated Unlearning

Even if the unlearning dataset and the remaining dataset do not share the same individual examples, they may still contain overlapping learnable information at the informational level as shown in Figure 1. This raises a key question: **Should the unlearning process remove the overlapping information? We argue that overlapping or shared information should not be unlearned.**

4.1 Definitions

Formally, we define the information F that the parameter distribution Φ learned from the data distribution \mathbb{D} as:

$$F = I(\Phi; \mathbb{D}). \quad (2)$$

Therefore, we can define the information F_o that the parameter distribution Φ learned from the training dataset which includes the remaining dataset D_r and unlearning dataset D_u as:

$$F_o = I(\Phi; D_r, D_u) \quad (3)$$

where I is the mutual information. The F_o measures how much information $D_u \cup D_r$ provides about Φ .

Similarly, we know the information F_r that the parameter distribution Φ learned only from the remaining dataset D_r as:

$$F_r = I(\Phi; D_r). \quad (4)$$

Therefore, we may roughly understand that F_o represents the learned information of the original model Φ_G and F_r denotes the learned information of the retrained model Φ_{G_r} .

4.2 Federated Memorization Unlearning

Next, we seek to characterize the unlearning process from an information-theoretic perspective. The resulting change in information can be quantified by:

$$\begin{aligned} F_{gap} &= F_o - F_r = I(\Phi; D_r, D_u) - I(\Phi; D_r) \\ &= I(\Phi; D_u \mid D_r) \end{aligned} \quad (5)$$

where $I(\Phi; D_u \mid D_r)$ indicates the information that D_u could provide about Φ when D_r is given.

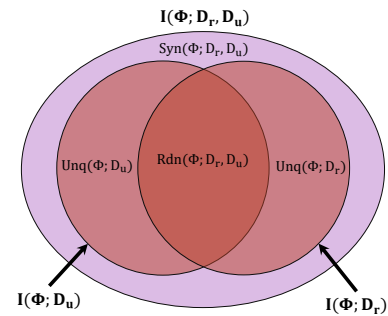


Figure 2: Structure of multivariate information for unlearning. Labelled regions correspond to unique information (Unq), redundancy (Rdn), and synergy (Syn).

According to the partial information decomposition [48] and Figure 2, $I(\Phi; D_r, D_u)$ actually include synergic information $Syn(\Phi; D_r, D_u)$

provided by D_r and D_u together, the unique information from D_r and D_u and the overlapping information $Rdn(\Phi; D_r, D_u)$ between D_r and D_u . We denote the overlapping information $Rdn(\Phi; D_r, D_u)$ as F_g , and the unique information $Unq(\Phi; D_u)$ from D_u as F_m . Consequently, $I(\Phi; D_u | D_r)$ corresponds to the combination of $Unq(\Phi; D_u)$ and $Syn(\Phi; D_r, D_u)$ shown in Figure 2. More specifically, $I(\Phi; D_u | D_r)$ comprises the synergistic information jointly provided by D_r and D_u , as well as the unique information contributed by D_u .

Thus, we formally propose our federated unlearning definition based on information theory:

DEFINITION 2. Federated Unlearning based on Information Theory. *Based on partial information decomposition, federated unlearning refers to the process of removing the information gap F_{gap} which includes synergistic information jointly provided by D_r and D_u and unique information of D_u . Given a global model Φ_G , the goal is to obtain an unlearned model Φ_{G_u} such that the influence of F_{gap} is effectively removed:*

$$\Phi_{G_u} \leftarrow A(\Phi_G, F_{gap}). \quad (6)$$

Furthermore, the unlearned model Φ_{G_u} should perform similarly to the retrained model Φ_{G_r} on the entire data distribution \mathbb{D} . This implies that we aim to develop an unlearning algorithm A and an unlearned model Φ_{G_u} that satisfy:

$$\Phi_{G_u} \leftarrow A(\Phi_G, F_{gap}) (\Phi_{G_u}(\mathbb{D})) \simeq \Phi_{G_r} \leftarrow f(D_r) (\Phi_{G_r}(\mathbb{D})), \quad (7)$$

where M denotes a measurement of output distribution similarity.

To demonstrate the impact of the synergistic component, we employ influence functions to analyze the parameter differences between the original model Φ_G and the retrained model Φ_{G_r} . Following Guo et al. [15], the effect of deleting D_u admits a first-order Newton approximation:

$$\Phi_{G_r} - \Phi_G = H_{\Phi_G}^{-1} \Delta + R, \quad (8)$$

where $H_{\Phi_G} = \nabla^2 L(\Phi_G, D_r)$ denotes the inverse Hessian evaluated on the retained dataset D_r , and $\Delta = \frac{1}{|D_r|} \sum_{(x,y) \in D_u} \nabla \ell(\Phi_G, (x, y))$ represents the aggregate gradient contribution of the deleted samples D_u . Moreover, R denotes the higher-order remainder term in the approximation. From this formulation, we observe that the aggregate gradient contribution of the deleted points D_u is the primary driver of the unlearning process. The synergistic information mainly resides in the higher-order remainder term R , which captures curvature changes and nonlinear effects along the optimization trajectory. Following the standard Lipschitz continuity assumption in related studies [15, 30], R can be safely neglected, implying that the synergistic information is minimal and the unlearning is predominantly governed by the unique information of D_u . This dominance of the unique information of D_u in the unlearning process is also consistent with intuition: unlearning mainly attempts to eliminate the influence of unlearning data.

Following this analysis, in practice, the synergistic information provided by D_r and D_u can be neglected and the unlearning should mainly remove the unique information of D_u , while preserving the overlapping information between D_r and D_u , to achieve the same information state as the retrained model. This type of unique information is exclusively provided by D_u , cannot be shared with

other data sources, but contributes to the model performance. Consequently, such unique information aligns with the definition of memorization [9, 10]. Thus, we can propose an approximate federated memorization unlearning definition:

DEFINITION 3. Federated Memorization Unlearning. *Based on Definition 2, we define federated memorization unlearning as an approximation of federated unlearning that primarily targets the memorization or unique information F_m of D_u when synergistic information provided by D_r and D_u can be neglected. Therefore, the information gap F_{gap} in unlearning can be represented as memorization information F_m of D_u :*

$$F_m \approx F_{gap} \quad (9)$$

Let Φ_G be the original federated model trained on $D_r \cup D_u$. In federated memorization unlearning, an unlearning algorithm A produces an unlearned model Φ_{G_u} intended to remove F_m from Φ_G . The unlearned model Φ_{G_u} should perform similarly to the retrained model Φ_{G_r} on the entire data distribution \mathbb{D} :

$$\Phi_{G_u} \leftarrow A(\Phi_G, F_m) (\Phi_{G_u}(\mathbb{D})) \simeq \Phi_{G_r} \leftarrow f(D_r) (\Phi_{G_r}(\mathbb{D})), \quad (10)$$

where M denotes a measurement of output distribution similarity.

5 Memorization-based Federated Unlearning Metrics

According to the discussion in Section 4, the partial information decomposition discloses that the primary difference between the unlearned model and the original model is that the unlearned model has removed the memorization information associated with the unlearning dataset. Thus, it is essential to verify the presence of memorization information to validate the unlearning results.

However, we find that existing metrics are insufficient for evaluating memorization in unlearning [42, 50].

In order to address this gap, we propose a novel unlearning metric specifically designed to evaluate memorization. **Direct evaluation of the memorization information F_m is challenging. Therefore, we move to the example level and indirectly assess whether the examples with memorization information have indeed been forgotten, to validate the unlearning process.**

Specifically, we develop an evaluation based on the memorization scores [9]. **Grouped Memorization Evaluation (GME)** aims to describe the performance of subgroups categorized by varying memorization scores within the unlearning dataset. GME consists of two steps: 1) Calculating unlearning memorization scores independently and grouping examples based on the scores; 2) Evaluating the performance of each subgroup on the unlearned model. The **Unlearning Memorization Score** of each example (x_i, y_i) in the unlearning dataset D_u can be determined using:

$$\text{mem}(f, D_r, D_u, (x_i, y_i)) = \Pr_{\Phi_G \leftarrow f(D_r \cup D_u)} [\Phi_G(x_i) = y_i] - \frac{1}{J} \sum_{j=1}^J \Pr_{\Phi_{G_r}^j \leftarrow f(D_r)} [\Phi_{G_r}^j(x_i) = y_i], \quad (11)$$

where D_u refers to the unlearning dataset, and D_r denotes the remaining dataset. To mitigate randomness, J retrained models Φ_{G_r} are generated without D_u , and the final measurement reflects the difference in the probability of correct classification, $\Pr[\Phi(x_i) = y_i]$, with and without the presence of D_u . **Generally, examples**

with high memorization scores contain more unique and memorization information.

Subsequently, the examples in the unlearning dataset D_u can be divided into different subgroups $\{T_p\}$ based on their memorization scores:

$$T_p = \{(x_i, y_i) \in D_u \mid \text{mem}_{(x_i, y_i)} \in (\tau_p, \tau_{p+1}]\}, \quad (12)$$

where τ is the predefined threshold and $(\tau_p, \tau_{p+1}]$ is the unlearning memorization score section of group T_p . In this work, we partition the subgroups by sorting the memorization scores from highest to lowest.

Next, we can apply any metric M (such as model accuracy) to evaluate the unlearning effect across different subgroups, as follows:

$$\Delta M_{T_p} = \left| \frac{M}{\Phi_{G_u \leftarrow A(\Phi_G, D_u)}}(\Phi_{G_u}, T_p) - \frac{M}{\Phi_{G_r \leftarrow f(D_r)}}(\Phi_{G_r}, T_p) \right| \quad (13)$$

where p denotes the index of the memorization subgroup T_p and ΔM_{T_p} is the unlearning difference on the specific subgroup T_p . Following Definition 3, we expect the unlearned model to perform similarly to the retrained model. Therefore, we aim for a minimal ΔM_{T_p} for each subgroup T_p . Evaluating these memorization score subgroups enables a more fine-grained assessment of the unlearning effect. In essence, examples with high memorization scores in D_u correspond to the memorization information F_m in our Definition 3. The common performance metrics can then be applied to these subgroups to more precisely characterize the effect of unlearning.

6 Federated Unlearning based on Memorization Pruning

6.1 Intuition

For a well-trained model, the information learned from data is encoded in its parameters. Based on the Definition 3, removing memorization information can achieve unlearning effectively. Therefore, pruning parameters that capture memorization information offers a potential unlearning strategy. This comes the first question: how to locate the memorization information in the parameter space. Previous studies [43] have identified important parameters relevant to unlearning dataset, based on large gradients and activations. However, these important parameters may capture both overlapping information F_g and memorization information F_m in the unlearning dataset D_u . In contrast, we hypothesize that redundant parameters with respect to the remaining dataset D_r appear to retain memorization information unique to the unlearning dataset D_u . The redundant parameters refer to the parameters that are not important with respect to the remaining dataset D_r and may correspond to F_m . We do not claim that redundant parameters exclusively encode F_m . Rather, we empirically observe that memorized information F_m of the unlearning clients is more concentrated in parameters that are less important to the remaining data, and we provide relevant discussion in Section 7.4. After pruning, the model Φ_{G_u} requires post fine-tuning on the remaining dataset to reconstruct the learned representations, as the pruning process directly disrupts the original representational structure.

6.2 FedMemPrune

The Federated Memorization Pruning (FedMemPrune) is a federated unlearning method that focuses on eliminating memorization.

In general, our approach comprises three stages: locating memorization parameters, resetting memorization parameters, and fine-tuning the network on the remaining dataset.

Overview. In the locating stage, we utilize the average gradient updates from the remaining clients to identify redundant parameters with minimal updates. Next, we employ the original initialization method to reset the memorization parameters. Finally, we fine-tune the unlearned model on the remaining clients to restore generalization performance. We present the algorithm in Appendix D.

Stage 1: Memorization location. As discussed in intuition, redundant or infrequently updated parameters are prone to retain memorization information. Therefore, we define the set of memorization parameters Θ_{um} as:

$$\Theta_{um} = \{\theta \in \Phi_G \mid \bar{g}_r(\theta) < \gamma\}, \quad (14)$$

where θ denotes a parameter in the global model Φ_G , $\bar{g}_r(\theta)$ represents the average gradient update of parameter θ , and γ is a predefined gradient threshold. The average gradient update $\bar{g}_r(\theta)$ is computed by aggregating the gradients submitted by the remaining clients, and is given by:

$$\bar{g}_r = \frac{1}{|K_r|} \sum_{k \in K_r} g_k, \quad (15)$$

where K_r denotes the index set of remaining clients and g_k is the gradient update of client k .

In practice, the threshold γ is determined based on a predefined percentage ρ of parameters to be reinitialized. Hence, ρ serves as the main hyperparameter in controlling unlearning.

Stage 2: Memorization parameters re-initialization. Since memorization information may not be completely removed by some optimization technologies, we directly choose to reset the memorization parameters. Rather than setting these parameters to zero, we reinitialize them using the original parameter initialization strategy. Specifically, we apply Kaiming Uniform Initialization [18] to the convolutional layers and the linear layers.

Stage 3: Fine-tuning on the remaining dataset. The final fine-tuning stage follows the standard training procedure, except that only the remaining clients participate. At the t' -th round of fine-tuning, the model aggregation is expressed as:

$$\Phi'_{G_u} = \frac{1}{|K_r|} \sum_{k \in K_r} \Phi'_k, \quad (16)$$

where Φ'_k denotes the local model of client k at round t' , and K_r is the index set of remaining clients.

The final global model Φ_{G_u} is the unlearned model, which effectively removes the influence of the unlearned clients while preserving the generalization performance.

7 Experiment

7.1 Experiment Setup

Dataset and Model Architecture. We evaluate our methods on three benchmark datasets: CIFAR-100, CIFAR-10 [25], EMNIST [6].

For CIFAR-100 and CIFAR-10, we employ a ResNet-34 model and ResNet-18 model [19]. EMNIST is processed using a VGG-9 model [40].

Baselines. During the evaluation, we select Halimi et al. [16], Liu et al. [30], FedRecovery [52], FedAU [14], FedOSD [34] and NoT [23] as the baselines. More detailed information can be found in Appendix E.1.

Evaluation Methods. We evaluate federated unlearning along four key dimensions: 1) **Unlearning Efficacy:** we employ Grouped Memorization Evaluation as discussed in Section 5 to quantify the effectiveness of unlearning; 2) **Generalization Performance:** we measure model test accuracy to assess generalization performance; 3) **Local Fairness:** we apply local fairness [37] as the degree to which the utility changes of remaining clients deviate from their average after unlearning, where lower variance indicates fairer outcomes. 4) **Time Analysis:** we examine how test performance changes during unlearning and compare it with the trajectory observed under full retraining along the time dimension. We provide specific explanation in Appendix E.2.

Implementation Details. We adopt the FedAvg framework with 10 clients. Our experiments focus on the case where a single client requests unlearning, under both IID and Non-IID settings. For the Non-IID case, we follow previous work [11, 41] and partition data using a Dirichlet distribution with concentration parameter $\alpha = 0.5$. More details of the implementation can be found in the Appendix E.3.

7.2 Evaluation Results

Unlearning Performance. Table 1 presents the performance of the unlearned model Φ_{G_u} , produced by different unlearning algorithms, across various memorization subgroups within the local dataset D_u of the unlearning client. Basically, this table directly demonstrate that our method most closely approximates the performance of the retrained model, particularly within the subgroup with the highest memorization scores. For example, in the evaluation of CIFAR-100 under Non-IID conditions, the classification accuracies of the retrained model Φ_{G_r} across the five memorization subgroups are 21.74%, 22.90%, 26.09%, 29.13%, and 65.28%, respectively. In comparison, our method achieves accuracies of 27.25%, 27.39%, 29.71%, 30.43%, and 63.44% on the same subgroups. This highlights the underlying consistent classification patterns shared by our model and the retrained baseline. However, other unlearning baselines fall significantly short of the performance of the retrained model, particularly in high-memorization groups.

Generalization Performance. Table 1 also reports the generalization performance across datasets and distribution conditions. Across all scenarios, our method consistently achieves the highest test accuracy on D_{test} , demonstrating strong generalization. In CIFAR-100 IID, it reaches 63.33%, far surpassing all baselines. Similar trends appear in other settings, where our method outperforms other unlearning baselines and approaches the retrained baseline generalization performance. These results support Section 4: by removing only memorization while preserving overlapping information, our method enables effective unlearning without harming generalization.

Local Fairness. Local fairness measures the variance in loss changes across the remaining local datasets compared to their average after unlearning. A lower variance indicates that the unlearning process induces similar performance changes for all remaining clients, thereby ensuring unlearning fairness. Table 1 shows that our method achieves the highest fairness in several scenarios because it avoids deleting overlapping information, thereby preventing significant performance degradation for clients providing such overlapping information. Specifically, for CIFAR-10, we achieve fairness scores of 0.91×10^{-3} and 44.12×10^{-3} under IID and Non-IID conditions, respectively, compared to the retrained baselines 0.09×10^{-3} and 30.78×10^{-3} , also outperforming other baselines.

Time Analysis. Figure 3 illustrates the test accuracy dynamics in training epochs for both retraining and our proposed unlearning method. Compared to retraining, our unlearning method achieves the highest test accuracy in significantly less time, showing around 50% time improvement. This is especially notable in the CIFAR-100 IID scenario (Figure F4a), where our method rapidly converges in 20 epochs, while retraining methods take nearly four times longer to stabilize. These practical results illustrate the time efficiency of our method. For other baselines applying different methods, we qualitatively analyze time complexity. FedRecovery [52] is the fastest because it utilize historical data, trading space for time. In the case of FedAU [14], it retrains only the final classification layer, which requires minimal computation time. In contrast, the method proposed by Liu et al. [30] employs a complex optimization procedure, demanding more time. Finally, both the methods of Halimi et al. [16] and FedOSD [34] include a post-training stage, resulting in a similar time consumption compared to our approach.

7.3 Ablation Studies

We conduct ablation experiments to analyze the factors influencing FedMemPrune.

Effect of Pruning Ratio. Fine-tuning alone ($\rho = 0\%$) fails to unlearn, leaving large accuracy gaps in high-memorization groups. A moderate pruning ratio ($\rho = 40\%$) achieves performance close to retraining with a 50% time improvement. The high pruning ($\rho \geq 60\%$) may cause excessive forgetting and converge toward retraining time and behavior. More details have been provided in Appendix F.1.

Effect of Data Distribution. Our method remains robust across diverse Non-IID settings, matching retraining performance. Notably, only fine-tuning suffices for unlearning when no information overlaps between unlearning and remaining dataset. See Appendix F.2 for details.

Impact of Parameter Selection Strategy. We compare our redundant parameter selection strategy with other parameter selection strategies [8, 43]. The results indicate that our strategy achieves a better balance between generalization performance and unlearning performance. Detailed results are provided in Appendix F.3.

Impact of Unlearning Multiple Clients. We demonstrate that our method remains effective when multiple clients request unlearning. We provide detailed results in Appendix F.4.

Table 1: Performance comparison of FedMemPrune vs. retrained and other baseline models

	Accuracy by Unlearning Memorization Score Subgroup (%) ($\Delta \downarrow$)					Unlearning Dataset Acc. (%) ($\Delta \downarrow$)	Test Dataset Acc. (%) \uparrow	Local Fairness (10^{-3}) \downarrow
	Group (95%,100%]	Group (90%,95%]	Group (85%,90%]	Group (80%,85%]	Group (0%,80%]			
CIFAR-100 IID								
Halimi et al.	51.47 \pm 0.19 (28.27)	54.93 \pm 0.19 (27.86)	52.93 \pm 0.19 (16.53)	55.20 \pm 0.00 (7.60)	82.77 \pm 0.11 (8.37)	78.89 \pm 0.09 (2.48)	52.56 \pm 0.05	23.83 \pm 0.08
Liu et al.	47.47 \pm 0.68 (24.27)	43.60 \pm 2.14 (16.53)	50.80 \pm 1.99 (14.40)	55.07 \pm 2.12 (7.47)	87.52 \pm 1.09 (3.62)	81.99 \pm 1.08 (0.62)	57.17 \pm 0.97	7.41 \pm 1.53
FedRecovery	60.67 \pm 3.94 (37.47)	61.60 \pm 2.14 (34.53)	57.87 \pm 0.68 (21.47)	58.40 \pm 1.18 (10.80)	86.70 \pm 0.58 (4.44)	83.22 \pm 0.58 (1.85)	55.01 \pm 0.23	7.83 \pm 2.39
FedAU	59.87 \pm 1.47 (36.67)	59.73 \pm 1.51 (32.66)	62.53 \pm 1.91 (26.13)	60.13 \pm 3.79 (12.53)	86.60 \pm 1.34 (4.54)	83.04 \pm 0.97 (1.67)	53.15 \pm 0.02	7.26 \pm 1.09
FedOSD	54.00 \pm 1.18 (30.80)	47.87 \pm 1.32 (20.80)	52.53 \pm 3.35 (16.13)	57.20 \pm 2.04 (9.60)	85.72 \pm 0.50 (5.42)	81.21 \pm 0.51 (0.16)	58.55 \pm 0.14	7.67 \pm 0.21
NoT	54.80 \pm 2.04 (31.60)	55.33 \pm 1.36 (28.26)	53.20 \pm 1.31 (16.80)	50.93 \pm 1.15 (3.33)	83.18 \pm 0.99 (7.96)	79.79 \pm 1.03 (1.58)	54.72 \pm 0.49	10.85 \pm 0.94
Ours	30.80 \pm 0.86 (7.60)	28.67 \pm 1.64 (1.60)	39.20 \pm 1.73 (2.80)	48.53 \pm 2.22 (0.93)	89.47 \pm 0.27 (1.67)	80.80 \pm 0.24 (0.57)	63.33 \pm 0.31	5.20 \pm 1.36
Retrained Baseline	23.20 \pm 9.62	27.07 \pm 5.85	36.40 \pm 2.90	47.60 \pm 1.18	91.14 \pm 0.68	81.37 \pm 0.51	62.29 \pm 0.58	6.46 \pm 1.81
CIFAR-100 Non-IID								
Halimi et al.	50.87 \pm 5.71 (29.13)	43.04 \pm 5.91 (20.14)	45.80 \pm 3.69 (19.71)	46.23 \pm 4.85 (17.10)	64.16 \pm 3.52 (1.12)	64.08 \pm 3.80 (2.78)	61.92 \pm 1.17	87.06 \pm 13.33
Liu et al.	43.33 \pm 0.41 (21.59)	36.09 \pm 1.55 (13.19)	34.35 \pm 0.35 (8.26)	33.48 \pm 1.42 (4.35)	64.07 \pm 0.85 (1.21)	61.73 \pm 0.92 (0.43)	58.02 \pm 0.55	54.98 \pm 8.93
FedRecovery	42.90 \pm 3.02 (21.16)	42.17 \pm 3.09 (19.27)	42.61 \pm 5.64 (16.52)	42.17 \pm 3.60 (13.04)	61.72 \pm 3.32 (3.56)	60.93 \pm 3.12 (0.37)	48.02 \pm 0.69	110.96 \pm 21.35
FedAU	52.46 \pm 1.96 (30.72)	47.54 \pm 1.79 (24.64)	41.30 \pm 2.22 (15.21)	39.42 \pm 5.96 (10.29)	57.43 \pm 2.57 (7.85)	56.75 \pm 2.07 (4.55)	46.68 \pm 0.97	71.90 \pm 13.28
FedOSD	56.09 \pm 4.43 (34.35)	43.19 \pm 3.69 (20.29)	42.46 \pm 4.41 (16.37)	38.26 \pm 3.09 (9.13)	62.30 \pm 2.42 (2.98)	61.53 \pm 2.47 (0.23)	59.59 \pm 0.79	88.11 \pm 22.91
NoT	46.96 \pm 2.13 (25.22)	40.58 \pm 0.82 (17.68)	45.94 \pm 0.74 (19.85)	40.14 \pm 1.75 (11.01)	64.74 \pm 0.10 (0.54)	63.40 \pm 1.13 (2.10)	57.06 \pm 0.16	50.08 \pm 11.57
Ours	27.25 \pm 1.25 (5.51)	27.39 \pm 2.22 (4.49)	29.71 \pm 1.68 (3.62)	30.43 \pm 2.48 (1.30)	63.44 \pm 0.69 (1.84)	60.37 \pm 0.74 (0.93)	62.99 \pm 0.53	42.78 \pm 6.56
Retrained Baseline	21.74 \pm 9.33	22.90 \pm 8.58	26.09 \pm 4.00	29.13 \pm 1.28	65.28 \pm 1.22	61.30 \pm 0.26	63.89 \pm 0.28	23.92 \pm 5.25
CIFAR-10 IID								
Halimi et al.	58.27 \pm 0.19 (45.47)	82.27 \pm 0.19 (47.87)	92.13 \pm 0.38 (14.53)	94.00 \pm 0.33 (1.87)	97.84 \pm 0.07 (1.28)	94.89 \pm 0.04 (4.58)	74.72 \pm 0.09	6.74 \pm 0.05
Liu et al.	53.33 \pm 1.80 (40.53)	70.00 \pm 1.13 (35.60)	76.53 \pm 1.86 (1.07)	87.07 \pm 0.94 (5.06)	98.33 \pm 0.24 (0.79)	93.16 \pm 0.25 (2.85)	68.13 \pm 0.24	1.23 \pm 0.25
FedRecovery	73.87 \pm 4.76 (61.07)	85.47 \pm 3.30 (51.07)	91.87 \pm 3.60 (14.27)	94.27 \pm 1.64 (2.14)	97.51 \pm 0.99 (1.61)	95.55 \pm 1.35 (5.24)	70.81 \pm 0.82	8.73 \pm 2.47
FedAU	77.87 \pm 6.71 (61.07)	78.67 \pm 6.88 (44.27)	82.93 \pm 2.17 (5.33)	83.60 \pm 3.22 (8.53)	91.67 \pm 2.53 (7.45)	89.09 \pm 1.78 (1.22)	62.48 \pm 1.20	6.04 \pm 1.76
FedOSD	66.80 \pm 4.09 (54.00)	83.47 \pm 1.47 (49.07)	91.87 \pm 0.38 (14.27)	91.07 \pm 2.00 (1.06)	97.05 \pm 1.03 (2.07)	94.51 \pm 1.00 (4.20)	70.39 \pm 0.34	6.27 \pm 0.69
NoT	36.40 \pm 1.70 (23.60)	66.27 \pm 0.19 (31.87)	82.00 \pm 1.31 (4.40)	85.20 \pm 1.42 (6.93)	96.22 \pm 0.87 (2.90)	91.06 \pm 0.75 (0.75)	74.56 \pm 0.28	6.16 \pm 0.97
Ours	20.27 \pm 1.54 (7.47)	50.40 \pm 3.44 (16.00)	70.93 \pm 2.29 (6.67)	85.60 \pm 0.86 (6.53)	98.66 \pm 0.20 (0.46)	90.56 \pm 0.35 (0.25)	74.97 \pm 0.27	0.91 \pm 0.07
Retrained Baseline	12.80 \pm 9.34	34.40 \pm 19.80	77.60 \pm 14.71	92.13 \pm 5.58	99.12 \pm 0.62	90.31 \pm 0.16	74.79 \pm 0.38	0.09 \pm 0.01
CIFAR-10 Non-IID								
Halimi et al.	45.02 \pm 0.44 (32.87)	44.44 \pm 0.44 (23.78)	45.33 \pm 0.66 (19.78)	58.06 \pm 0.89 (15.65)	84.27 \pm 0.18 (7.89)	79.16 \pm 0.15 (1.25)	65.49 \pm 0.13	172.45 \pm 1.63
Liu et al.	73.68 \pm 13.07 (61.53)	61.97 \pm 13.91 (41.31)	61.21 \pm 11.47 (35.66)	61.35 \pm 9.64 (18.94)	88.94 \pm 4.81 (3.22)	84.94 \pm 5.88 (4.53)	68.22 \pm 2.71	219.91 \pm 103.08
FedRecovery	43.61 \pm 1.17 (31.46)	42.88 \pm 3.12 (22.22)	44.55 \pm 0.58 (19.00)	51.33 \pm 2.31 (8.92)	81.55 \pm 1.99 (10.61)	76.92 \pm 1.48 (3.49)	62.45 \pm 2.14	148.91 \pm 28.94
FedAU	77.10 \pm 11.57 (64.95)	67.45 \pm 8.10 (46.79)	69.00 \pm 4.62 (43.45)	69.17 \pm 3.56 (26.76)	85.24 \pm 4.83 (6.92)	82.38 \pm 5.32 (1.97)	61.38 \pm 0.49	107.94 \pm 46.10
FedOSD	73.68 \pm 4.19 (61.53)	61.50 \pm 1.01 (40.84)	61.37 \pm 0.79 (35.82)	66.67 \pm 1.01 (24.26)	94.38 \pm 0.53 (2.22)	89.18 \pm 0.43 (8.77)	73.59 \pm 0.18	80.27 \pm 1.17
NoT	30.22 \pm 0.44 (18.07)	36.62 \pm 1.01 (15.96)	43.15 \pm 0.58 (17.60)	55.87 \pm 1.01 (13.46)	88.15 \pm 0.67 (4.01)	80.74 \pm 0.45 (0.33)	72.16 \pm 0.78	76.15 \pm 12.65
Ours	23.99 \pm 2.86 (11.84)	27.86 \pm 1.81 (7.20)	39.72 \pm 0.66 (14.17)	47.57 \pm 2.18 (5.16)	88.80 \pm 1.17 (3.36)	80.16 \pm 0.81 (0.25)	74.43 \pm 0.78	44.12 \pm 5.20
Retrained Baseline	12.15 \pm 8.80	20.66 \pm 14.61	25.55 \pm 18.07	42.41 \pm 10.43	92.16 \pm 4.27	80.41 \pm 0.09	74.93 \pm 0.32	30.78 \pm 6.58
EMNIST IID								
Halimi et al.	66.67 \pm 0.98 (19.28)	86.06 \pm 0.42 (12.16)	95.56 \pm 0.34 (4.27)	97.72 \pm 0.08 (2.28)	99.80 \pm 0.04 (0.20)	96.67 \pm 0.11 (0.57)	92.64 \pm 0.03	2.85 \pm 0.05
Liu et al.	62.22 \pm 1.70 (14.83)	90.50 \pm 1.47 (7.72)	98.83 \pm 0.00 (1.00)	99.17 \pm 0.24 (0.83)	100.00 \pm 0.00 (0.00)	97.13 \pm 0.18 (0.11)	92.90 \pm 0.05	5.30 \pm 0.54
FedRecovery	74.78 \pm 0.75 (27.39)	89.17 \pm 0.76 (9.05)	96.11 \pm 0.86 (3.72)	98.11 \pm 0.34 (1.89)	99.77 \pm 0.10 (0.23)	97.32 \pm 0.12 (0.08)	92.56 \pm 0.05	2.61 \pm 0.59
FedAU	69.56 \pm 3.68 (22.17)	84.83 \pm 3.08 (13.39)	89.00 \pm 3.09 (10.83)	93.94 \pm 1.23 (6.06)	98.78 \pm 0.41 (1.22)	94.21 \pm 0.81 (3.03)	88.57 \pm 0.47	3.29 \pm 0.21
FedOSD	69.06 \pm 1.88 (21.67)	87.67 \pm 2.13 (10.55)	96.61 \pm 1.85 (3.22)	97.61 \pm 1.11 (2.39)	99.87 \pm 0.12 (0.13)	96.73 \pm 0.65 (0.51)	92.62 \pm 0.40	2.85 \pm 0.22
NoT	48.50 \pm 0.14 (11.11)	75.33 \pm 1.06 (22.89)	91.11 \pm 0.08 (8.72)	96.67 \pm 0.00 (3.33)	99.66 \pm 0.00 (0.34)	94.45 \pm 0.05 (2.79)	92.62 \pm 0.04	4.04 \pm 0.03
Ours	53.06 \pm 1.86 (5.67)	94.33 \pm 0.85 (3.89)	99.50 \pm 0.14 (0.33)	99.83 \pm 0.00 (0.17)	99.97 \pm 0.02 (0.03)	97.19 \pm 0.11 (0.05)	93.50 \pm 0.06	0.70 \pm 0.15
Retrained Baseline	47.39 \pm 1.95	98.22 \pm 1.23	99.83 \pm 0.14	100.00 \pm 0.00	100.00 \pm 0.00	97.24 \pm 0.01	93.60 \pm 0.01	0.18 \pm 0.03
EMNIST Non-IID								
Halimi et al.	58.13 \pm 0.20 (37.56)	64.69 \pm 0.15 (2.22)	79.33 \pm 0.21 (8.63)	94.78 \pm 0.06 (2.30)	99.25 \pm 0.01 (0.58)	93.48 \pm 0.02 (0.58)	88.82 \pm 0.01	45.02 \pm 1.24
Liu et al.	49.88 \pm 6.62 (29.31)	64.04 \pm 6.05 (2.87)	84.87 \pm 3.43 (3.09)	95.93 \pm 1.57 (1.15)	99.76 \pm 0.11 (0.07)	93.56 \pm 1.04 (0.50)	88.75 \pm 0.46	136.33 \pm 41.18
FedRecovery	67.00 \pm 9.32 (46.43)	77.64 \pm 9.97 (10.73)	87.92 \pm 4.45 (0.04)	95.68 \pm 0.87 (1.40)	99.62 \pm 0.15 (0.21)	95.60 \pm 1.62 (2.62)	87.80 \pm 0.57	46.23 \pm 20.40
FedAU	69.95 \pm 7.48 (49.38)	67.37 \pm 6.25 (0.46)	84.55 \pm 4.80 (3.41)	95.97 \pm 2.06 (1.11)	99.78 \pm 0.09 (0.05)	94.43 \pm 1.43 (1.45)	87.60 \pm 0.98	31.94 \pm 16.40
FedOSD	57.55 \pm 7.34 (36.98)	64.98 \pm 6.20 (1.93)	85.49 \pm 3.92 (2.47)	96.22 \pm 1.62 (0.86)	99.80 \pm 0.03 (0.03)	93.93 \pm 1.18 (0.95)	88.99 \pm 0.40	58.99 \pm 12.85
NoT	38.88 \pm 0.25 (18.31)	65.23 \pm 0.17 (1.68)	86.07 \pm 0.70 (1.89)	95.77 \pm 0.15 (1.31)	99.80 \pm 0.01 (0.03)	93.37 \pm 0.04 (0.39)	89.30 \pm 0.03	22.64 \pm 3.81
Ours	33.33 \pm 0.76 (12.76)	63.50 \pm 1.43 (3.41)	85.45 \pm 1.22 (2.51)	96.59 \pm 0.06 (0.49)	99.80 \pm 0.01 (0.03)	93.16 \pm 0.24 (0.18)	89.21 \pm 0.10	19.35 \pm 1.41
Retrained Baseline	20.57 \pm 13.60	66.91 \pm 6.01	87.96 \pm 2.41	97.08 \pm 0.71	99.83 \pm 0.04	92.98 \pm 0.17	89.18 \pm 0.06	18.73 \pm 2.73

We report accuracies of the unlearned model Φ_{G_u} on memorization subgroups T_p of the unlearning dataset D_u and the test dataset D_{test} , along with the local fairness metric. Subgroups are defined by percentile ranges of unlearning memorization scores (e.g., (95%, 100%] contains the top 5% memorization examples). Accuracy differences Δ from retrained baselines are shown in blue, with the smallest differences and the best test, fairness performance highlighted in red.

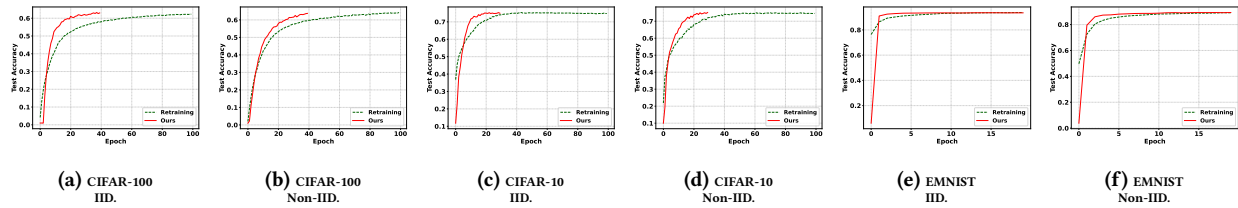


Figure 3: Efficiency comparison between unlearning and retraining.

Impact of Large Scale FL Setting. We demonstrate that our method performs well in federated learning scenarios with a larger number of clients. Detailed results are provided in Appendix F.5.

7.4 Discussion

Relationship between Parameters and Information. We attempt to investigate the relationship between parameters and information representation. Our experiments show that important parameters mainly encode overlapping/generalized information, whereas redundant parameters are more closely tied to memorization. The results are presented in Appendix H.1.

Pruning Ratio Selection. The pruning ratio ρ is a key hyperparameter in our method. Accordingly, we propose a method to select the pruning ratio ρ based on the proportion of redundant parameters. Given the sparsity of parameters in neural networks, it is feasible to determine a threshold of small magnitude based on parameter importance to achieve the desired pruning ratio. Further details are provided in Appendix H.2.

Extending to Class-Level and Example-Level Unlearning. We evaluate our approach on both class-level and example-level unlearning tasks. Our method can be seamlessly applied to class-level unlearning and demonstrates strong performance in this setting. For example-level unlearning, the system may accumulate multiple single-example unlearning requests before executing the unlearning pipeline. Therefore, example-level unlearning is similar to client-level unlearning. Our approach continues to perform effectively in this setting. A detailed discussion is provided in Appendix H.3.

Loss surface of the shortest unlearning path. We examine the loss surface of the shortest unlearning path. The analysis reveals that the original and retrained models lie in different loss basins. Even small perturbations to the original parameters sharply increase loss. This implies that unlearning is inherently closer to a partial re-training process, highlighting the necessity of performance recovery. We provided details in Appendix H.4.

8 Conclusion

By distinguishing between overlapping and memorization information, we argue that effective unlearning should target only memorization information, preserving model generalization and the contributions of other clients. To this end, we introduced FedMemPrune, a novel approach that selectively removes memorization parameters, achieving robust and efficient unlearning. Our findings

offer both theoretical insights and practical strategies for strengthening federated unlearning.

References

- [1] Julius Adebayo, Justin Gilmer, Michael Muelly, Ian Goodfellow, Moritz Hardt, and Been Kim. 2018. Sanity Checks for Saliency Maps. In *Advances in Neural Information Processing Systems*, S. Bengio, H. Wallach, H. Larochelle, K. Grauman, N. Cesa-Bianchi, and R. Garnett (Eds.), Vol. 31. Curran Associates, Inc. https://proceedings.neurips.cc/paper_files/paper/2018/file/294a8ed24b1ad22ec2e7efea049b8737-Paper.pdf
- [2] Lucas Bourtole, Varun Chandrasekaran, Christopher A Choquette-Choo, Hengrui Jia, Adelin Travers, Baiwu Zhang, David Lie, and Nicolas Papernot. 2021. Machine unlearning. In *2021 IEEE Symposium on Security and Privacy (SP)*. IEEE, 141–159. doi:10.1109/SP40001.2021.00019
- [3] Yinzhi Cao and Junfeng Yang. 2015. Towards making systems forget with machine unlearning. In *2015 IEEE Symposium on Security and Privacy (SP)*. IEEE, 463–480. doi:10.1109/SP.2015.35
- [4] Nicolas Carlini, Jamie Hayes, Milad Nasr, Matthew Jagielski, Vikash Shwag, Florian Tramèr, Borja Balle, Daphne Ippolito, and Eric Wallace. 2023. Extracting Training Data from Diffusion Models. In *32nd USENIX Security Symposium (USENIX Security 23)*. 5253–5270.
- [5] Nicholas Carlini, Chang Liu, Úlfar Erlingsson, Jernej Kos, and Dawn Song. 2019. The secret sharer: Evaluating and testing unintended memorization in neural networks. In *28th USENIX security symposium (USENIX security 19)*. 267–284.
- [6] Gregory Cohen, Saeed Afshar, Jonathan Tappan, and Andre Van Schaik. 2017. EMNIST: Extending MNIST to handwritten letters. In *2017 international joint conference on neural networks (IJCNN)*. IEEE, 2921–2926. doi:10.1109/IJCNN.2017.7966217
- [7] Zhipeng Deng, Luyang Luo, and Hao Chen. 2024. Enable the right to be forgotten with federated client unlearning in medical imaging. In *International Conference on Medical Image Computing and Computer-Assisted Intervention (MICCAI)*. Springer, 240–250. doi:10.1007/978-3-031-72117-5_23
- [8] Chongyu Fan, Jiancheng Liu, Yihua Zhang, Dennis Wei, Eric Wong, and Sijia Liu. 2024. SaUn: Empowering Machine Unlearning via Gradient-Based Weight Saliency in Both Image Classification and Generation. In *International Conference on Learning Representations (ICLR)*.
- [9] Vitaly Feldman. 2020. Does learning require memorization? a short tale about a long tail. In *Proceedings of the 52nd Annual ACM SIGACT Symposium on Theory of Computing (STOC 2020)*. Association for Computing Machinery, New York, NY, USA, 954–959. doi:10.1145/3357713.3384290
- [10] Vitaly Feldman and Chiyuan Zhang. 2020. What Neural Networks Memorize and Why: Discovering the Long Tail via Influence Estimation. In *Advances in Neural Information Processing Systems*, Vol. 33. Curran Associates, Inc., 2881–2891.
- [11] Xiangshan Gao, Xingjun Ma, Jingyi Wang, Youcheng Sun, Bo Li, Shouling Ji, Peng Cheng, and Jiming Chen. 2024. Verifi: Towards verifiable federated unlearning. *IEEE Transactions on Dependable and Secure Computing* (2024). doi:10.1109/TDSC.2024.3382321
- [12] Aditya Golatkar, Alessandro Achille, and Stefano Soatto. 2020. Eternal sunshine of the spotless net: Selective forgetting in deep networks. In *Proceedings of the IEEE/CVF conference on computer vision and pattern recognition*. 9304–9312. doi:10.1109/CVPR42600.2020.00932
- [13] Ian J Goodfellow, Mehdi Mirza, Da Xiao, Aaron Courville, and Yoshua Bengio. 2013. An empirical investigation of catastrophic forgetting in gradient-based neural networks. *arXiv preprint arXiv:1312.6211* (2013).
- [14] Hanlin Gu, Gongxi Zhu, Jie Zhang, Xinyuan Zhao, Yuxing Han, Lixin Fan, and Qiang Yang. 2024. Unlearning during learning: an efficient federated machine unlearning method. In *Proceedings of the Thirty-Third International Joint Conference on Artificial Intelligence*. 4035–4043.
- [15] Chuan Guo, Tom Goldstein, Awini Hannun, and Laurens Van Der Maaten. 2020. Certified data removal from machine learning models. In *Proceedings of the 37th International Conference on Machine Learning*. PMLR.

- [16] Anisa Halimi, Swanand Ravindra Kadhe, Ambrish Rawat, and Nathalie Baracaldo Angel. 2022. Federated Unlearning: How to Efficiently Erase a Client in FL?. In *International Conference on Machine Learning*.
- [17] Elizabeth Liz Harding, Jarno J Vanto, Reece Clark, L Hannah Ji, and Sara C Ainsworth. 2019. Understanding the scope and impact of the california consumer privacy act of 2018. *Journal of Data Protection & Privacy* 2, 3 (2019), 234–253.
- [18] Kaiming He, Xiangyu Zhang, Shaoqing Ren, and Jian Sun. 2015. Delving deep into rectifiers: Surpassing human-level performance on imagenet classification. In *Proceedings of the IEEE international conference on computer vision*. 1026–1034. doi:10.1109/ICCV.2015.123
- [19] Kaiming He, Xiangyu Zhang, Shaoqing Ren, and Jian Sun. 2016. Deep residual learning for image recognition. In *Proceedings of the IEEE conference on computer vision and pattern recognition*. 770–778. doi:10.1109/CVPR.2016.90
- [20] Joel Jang, Dongkeun Yoon, Sohee Yang, Sungmin Cha, Moontae Lee, Lajanugen Logeswaran, and Minjoon Seo. 2023. Knowledge unlearning for mitigating privacy risks in language models. In *Proceedings of the 61st Annual Meeting of the Association for Computational Linguistics (Volume 1: Long Papers)*. 14389–14408. doi:10.18653/v1/2023.acl-long.805
- [21] Hyejun Jeong, Shiqing Ma, and Amir Houmansadr. 2024. Sok: Challenges and opportunities in federated unlearning. *arXiv preprint arXiv:2403.02437* (2024). doi:10.48550/ARXIV.2403.02437
- [22] Peter Kairouz, H Brendan McMahan, Brendan Avent, Aurélien Bellet, Mehdi Bennis, Arjun Nitin Bhagoji, Kallista Bonawitz, Zachary Charles, Graham Cormode, Rachel Cummings, et al. 2021. Advances and open problems in federated learning. *Foundations and trends® in machine learning* 14, 1–2 (2021), 1–210. doi:10.1561/22000000083
- [23] Yasser H Khalil, Leo Brunswic, Soufiane Lamghari, Xu Li, Mahdi Beitollahi, and Xi Chen. 2025. NoT: Federated Unlearning via Weight Negation. In *Proceedings of the Computer Vision and Pattern Recognition Conference*. 25759–25769. doi:10.1109/CVPR52734.2025.02399
- [24] Jakub Konečný, H. Brendan McMahan, Daniel Ramage, and Peter Richtárik. 2016. Federated Optimization: Distributed Machine Learning for On-Device Intelligence. doi:10.48550/arXiv.1610.02527
- [25] Alex Krizhevsky, Geoffrey Hinton, et al. 2009. Learning multiple layers of features from tiny images. (2009).
- [26] Na Li, Chunyi Zhou, Yansong Gao, Hui Chen, Zhi Zhang, Boyu Kuang, and Anmin Fu. 2025. Machine unlearning: Taxonomy, metrics, applications, challenges, and prospects. *IEEE Transactions on Neural Networks and Learning Systems* (2025). doi:10.1109/TNNLS.2025.3530988
- [27] Yuyuan Li, Chaochao Chen, Xiaolin Zheng, and Jiaming Zhang. 2023. Federated unlearning via active forgetting. *arXiv preprint arXiv:2307.03363* (2023).
- [28] Yijing Lin, Zhipeng Gao, Hongyang Du, Jinke Ren, Zhiqiang Xie, and Dusit Niyato. 2024. Blockchain-enabled trustworthy federated unlearning. *arXiv preprint arXiv:2401.15917* (2024).
- [29] Gaoyang Liu, Xiaoqiang Ma, Yang Yang, Chen Wang, and Jiangchuan Liu. 2021. Federaser: Enabling efficient client-level data removal from federated learning models. In *2021 IEEE/ACM 29th International Symposium on Quality of Service (IWQOS)*. IEEE, 1–10. doi:10.1109/IWQOS52092.2021.9521274
- [30] Yi Liu, Lei Xu, Xingliang Yuan, Cong Wang, and Bo Li. 2022. The right to be forgotten in federated learning: An efficient realization with rapid retraining. In *IEEE INFOCOM 2022-IEEE Conference on Computer Communications*. IEEE, 1749–1758. doi:10.1109/INFOCOM48880.2022.9796721
- [31] Ziyao Liu, Yu Jiang, Jiyuan Shen, Minyi Peng, Kwok-Yan Lam, Xingliang Yuan, and Xiaoning Liu. 2024. A survey on federated unlearning: Challenges, methods, and future directions. *Comput. Surveys* 57, 1 (2024), 1–38. doi:10.1145/3679014
- [32] Pratyush Maini, Michael Curtis Mozer, Hanie Sedghi, Zachary Chase Lipton, J Zico Kolter, and Chiyuan Zhang. 2023. Can Neural Network Memorization Be Localized?. In *International Conference on Machine Learning*. PMLR, 23536–23557.
- [33] Brendan McMahan, Eider Moore, Daniel Ramage, Seth Hampson, and Blaise Aguera y Arcas. 2017. Communication-Efficient Learning of Deep Networks from Decentralized Data. In *Proceedings of the 20th International Conference on Artificial Intelligence and Statistics*. PMLR, 1273–1282.
- [34] Zibin Pan, Zhichao Wang, Chi Li, Kaiyan Zheng, Boqi Wang, Xiaoying Tang, and Junhua Zhao. 2025. Federated unlearning with gradient descent and conflict mitigation. In *Proceedings of the AAAI Conference on Artificial Intelligence*, Vol. 39. 19804–19812. doi:10.1609/AAAI.V39I19.34181
- [35] Ramprasaath R Selvaraju, Michael Cogswell, Abhishek Das, Ramakrishna Vedantam, Devi Parikh, and Dhruv Batra. 2017. Grad-cam: Visual explanations from deep networks via gradient-based localization. In *Proceedings of the IEEE international conference on computer vision*. 618–626.
- [36] Thanveer Shaik, Xiaohui Tao, Lin Li, Haoran Xie, Taotao Cai, Xiaofeng Zhu, and Qing Li. 2024. FRAMU: Attention-based machine unlearning using federated reinforcement learning. *IEEE Transactions on Knowledge and Data Engineering* (2024).
- [37] Jiaqi Shao, Tao Lin, Xuanyu Cao, and Bing Luo. 2024. Federated unlearning: a perspective of stability and fairness. *arXiv preprint arXiv:2402.01276* (2024). doi:10.48550/ARXIV.2402.01276
- [38] Reza Shokri and Vitaly Shmatikov. 2015. Privacy-Preserving Deep Learning. In *Proceedings of the 22nd ACM SIGSAC Conference on Computer and Communications Security (CCS '15)*. Association for Computing Machinery, New York, NY, USA, 1310–1321. doi:10.1145/2810103.2813687
- [39] K Simonyan, A Vedaldi, and A Zisserman. 2014. Deep inside convolutional networks: visualising image classification models and saliency maps. *International Conference on Learning Representations*.
- [40] K Simonyan and A Zisserman. 2015. Very deep convolutional networks for large-scale image recognition. In *International Conference on Learning Representations (ICLR)*.
- [41] Ningxin Su and Baochun Li. 2023. Asynchronous federated unlearning. In *IEEE INFOCOM 2023-IEEE conference on computer communications*. IEEE, 1–10. doi:10.1109/INFOCOM53939.2023.10229075
- [42] Anvith Thudi, Hengrui Jia, Ilia Shumailov, and Nicolas Papernot. 2022. On the necessity of auditable algorithmic definitions for machine unlearning. In *31st USENIX security symposium (USENIX Security 22)*. 4007–4022.
- [43] Reihaneh Torkzadehmahani, Reza Nasirigerdeh, Georgios Kaissis, Daniel Rueckert, Gintare Karolina Dziugaite, and Eleni Triantafyllou. 2025. Improved Localized Machine Unlearning Through the Lens of Memorization. *Transactions on Machine Learning Research* (2025).
- [44] Paul Voigt and Axel von dem Bussche. 2017. *The EU General Data Protection Regulation (GDPR): A Practical Guide*. Springer International Publishing. doi:10.1007/978-3-319-57960-3
- [45] Junxiao Wang, Song Guo, Xin Xie, and Heng Qi. 2022. Federated unlearning via class-discriminative pruning. In *Proceedings of the ACM web conference*. 622–632. doi:10.1145/3485447.3512222
- [46] Weiqi Wang, Zhiyi Tian, Chenhan Zhang, An Liu, and Shui Yu. 2023. Bfu: Bayesian federated unlearning with parameter self-sharing. In *Proceedings of the 2023 ACM Asia Conference on Computer and Communications Security*. 567–578.
- [47] Weiqi Wang, Zhiyi Tian, Chenhan Zhang, and Shui Yu. 2024. Machine unlearning: A comprehensive survey. *arXiv preprint arXiv:2405.07406* (2024).
- [48] Paul L Williams and Randall D Beer. 2010. Nonnegative decomposition of multivariate information. *arXiv preprint arXiv:1004.2515* (2010).
- [49] Chen Wu, Sencun Zhu, and Prasenjit Mitra. 2022. Federated unlearning with knowledge distillation. *arXiv preprint arXiv:2201.09441* (2022).
- [50] Binchi Zhang, Zihan Chen, Cong Shen, and Jundong Li. 2024. Verification of machine unlearning is fragile. (2024), 58717–58738.
- [51] Chiyuan Zhang, Samy Bengio, Moritz Hardt, Benjamin Recht, and Oriol Vinyals. 2021. Understanding deep learning (still) requires rethinking generalization. *Commun. ACM* 64, 3 (2021), 107–115. doi:10.1145/3446776
- [52] Lefeng Zhang, Tianqing Zhu, Haibin Zhang, Ping Xiong, and Wanlei Zhou. 2023. Fedrecovery: Differentially private machine unlearning for federated learning frameworks. *IEEE Transactions on Information Forensics and Security* 18 (2023), 4732–4746. doi:10.1109/TIFS.2023.3297905
- [53] Yian Zhao, Pengfei Wang, Heng Qi, Jianguo Huang, Zongzheng Wei, and Qiang Zhang. 2023. Federated unlearning with momentum degradation. *IEEE Internet of Things Journal* 11, 5 (2023), 8860–8870. doi:10.1109/JIOT.2023.3321594

Appendix A Statement on the Use of Large Language Models (LLMs)

The authors confirm that large language models were used only for text improvement purposes (including grammar, clarity, and stylistic refinement). No part of the conceptual development, experimental design, analysis, or substantive content of the paper relied on LLM assistance. All scientific contributions are entirely the work of the authors.

Appendix B Reproducibility statement

For reproducibility, we provide detailed descriptions of datasets, model architectures in the main text. Moreover, we provide the algorithm in Appendix D and implement details in Appendix E.3. Additionally, we provide our code in <https://github.com/JWei1999/Rethinking-Federated-Unlearning-via-the-Lens-of-Memorization>.

Appendix C Notations

Table C1: Table of notations.

Symbol	Description
K	The set of client indices.
K_u	The set of unlearning client indices.
K_r	The set of remaining client indices.
C_k	The client corresponding to index k .
\mathbb{D}	The underlying data distribution.
D_k	The local private dataset of the client with index k .
D	The set of all local datasets from all clients.
D_u	The set of all local datasets from unlearning clients with indices in K_u .
D_r	The set of all local datasets from remaining clients with indices in K_r .
D_{rest}	The test dataset that simulates the unseen data.
f	The federated learning algorithm.
A	The federated unlearning algorithm.
Φ_G	The global model.
Φ_{G_u}	The global unlearned model.
Φ_{G_r}	The global retrained model.
M	The performance measurement method, e.g., accuracy.
$F_g(\Phi)$	The overlapped information that Φ learns from both D_u and D_r .
$F_m(\Phi)$	The non-overlapping information that Φ only learn from D_u .
τ	The pre-defined threshold to split memorization score groups.
T_p	The group of examples categorized by the memorization score at index p .
θ	The partial parameters in model Φ .
g_k	The gradient update of client C_k on its local dataset D_k .
γ	The predefined gradient threshold.
ρ	The predefined percentage gradient threshold.
α	The concentration parameter of a Dirichlet distribution.

Appendix D Algorithm Description

In this subsection, we give the completed pipeline of our unlearning method in Algorithm 1.

Appendix E Experiment Details

Appendix E.1 Baselines

In this subsection, we provide a detailed explanation of the unlearning baselines:

- **Halimi et al.** [16] This work attempts to revert the training process via gradient ascent. However, since gradient ascent can lead to an arbitrary model, the unlearned model is restricted within a predefined threshold in terms of the distance l_2 .
- **Liu et al.** [30] Liu et al. propose a method that leverages the Fisher Information Matrix (FIM) to estimate the inverse Hessian matrix and guide the unlearning process.

Algorithm 1 FedMemPrune

Input: Trained global model Φ_G ; remaining clients $\{C_k \mid k \in K_r\}$ and its index set K_r ; drop ratio ρ (or threshold γ); local learning rate λ .

Output: Unlearned model $\Phi_{G_u}^u$.

► **Stage 1: Locate memorization parameters.**

- 1: Server broadcasts Φ_G to all remaining client $\{C_k \mid k \in K_r\}$.
- 2: Initialize local model $\Phi_k \leftarrow \Phi_G$ for each client C_k that $k \in K_r$.
- 3: Calculate gradient update

$$g_k = \nabla_{\Phi_k} \mathcal{L}(\Phi_k, D_k)$$

for each client C_k in $\{C_k \mid k \in K_r\}$.

- 4: Compute average gradient of remaining clients $\{C_k \mid k \in K_r\}$:

$$\bar{g}_r = \frac{1}{|K_r|} \sum_{k \in K_r} g_k$$

- 5: Select *redundant parameters*:

$$\Theta_{um} = \{\theta \in \Phi_G \mid \bar{g}_r(\theta) < \gamma\},$$

or equivalently choose the lowest ρ parameters by $|g_r(\theta)|$.

► **Stage 2: Reset memorization parameters.**

- 6: Re-initialize Θ_{um} using the original scheme (e.g., Kaiming Uniform for conv/linear) and denote the reset model as $\Phi_{G_u}^0$.

► **Stage 3: Fine-tuning on remaining clients.**

- 7: **for** $t \leftarrow 0$ to t_{end} **do**
- 8: Server broadcasts $\Phi_{G_u}^t$ to remaining clients $\{C_k \mid k \in K_r\}$.
- 9: **for all** $k \in K_r$ **in parallel do**
- 10: $\Phi_k^{r0} \leftarrow \Phi_k^t$
- 11: **for** $r \leftarrow 0$ to r_{end} **do**
- 12: Update local model

$$\Phi_k^{r+1} = \Phi_k^r - \lambda \nabla_{\Phi_k^r} \mathcal{L}(\Phi_k^r, D_k).$$

- 13: **end for**

- 14: $\Phi_k^{t+1} \leftarrow \Phi_k^{r_{end}}$

- 15: **end for**

- 16: Compute average model of remaining clients $\{C_k \mid k \in K_r\}$:

$$\Phi_{G_u}^{t+1} = \frac{1}{|K_r|} \sum_{k \in K_r} \Phi_k^{t+1}$$

- 17: **end for**

- 18: $\Phi_{G_u} \leftarrow \Phi_{G_u}^{t_{end}}$

- 19: **return** Φ_{G_u}
-

- **FedRecovery**. [52] FedRecovery aims to reduce the updates related to unlearning data by utilizing historical update storage, and applies differential privacy to enhance indistinguishability compared to the retrained model.
- **FedAU**. [14] FedAU perturbs the learned features of unlearning data by employing random labels. Through linear operations, retraining the classification layer is a more efficient unlearning method.
- **FedOSD**. [34] FedOSD introduces advanced techniques to address gradient exploration during gradient ascent and gradient conflicts during unlearning, thereby mitigating model utility degradation.
- **NoT**. [23] NoT is a recent federated unlearning approach that aims to apply strong and resilient weight negation to model weights in order to induce unlearning and enable rapid recovery.

Appendix E.2 Evaluation Methods

Unlearning Efficacy. We employ Grouped Memorization Evaluation, as discussed in Section 6, to quantify the effectiveness of unlearning. In this experiment, we set $J = 3$ to mitigate randomness. Moreover, we divide the examples according to their memorization score percentiles: (95%, 100%], (90%, 95%], (85%, 90%], (80%, 85%], and (0%, 80%]. According to the long-tail theory [9, 10], only the tail portion corresponds to memorization examples. Consequently, we regard the top 20% of examples by memorization score, i.e., those in the (80%, 100%] range, as representing memorization information. The remaining examples, in the range (0%, 80%], are considered mainly carrying overlapping or generalizable information. To assess unlearning effectiveness, we compare the performance of the unlearned model to that of a retrained model. A smaller performance difference indicates more effective unlearning, particularly in terms of removing memorization information.

Generalization Performance. Generalization performance is typically evaluated using a test dataset. Accordingly, we use

$$\text{Accuracy}(\Phi_{G_u}, D_{test})$$

to assess the generalization capability of the model.

Local Fairness. Local fairness [37] in the context of federated unlearning is defined as the extent to which the utility changes of the remaining clients deviate from their average after unlearning. This definition ensures that the unlearning process induces similar performance variation across all remaining clients, thereby promoting fairness. The performance change for a client C_k is given by

$$\Delta L_k(\Phi_{G_u}) = L(\Phi_{G_u}, D_k) - L(\Phi_G, D_k).$$

The local fairness metric can then be expressed as

$$\text{LocalFairness}(\Phi_{G_u}) = \sum_{k \in K_r} \left| \Delta L_k(\Phi_{G_u}) - \overline{\Delta L} \right|,$$

where $\overline{\Delta L}$ is the average performance change across all remaining clients.

Time Analysis. We record the changes in generalization performance throughout the unlearning process and compare them with the performance trajectory observed during full retraining, with respect to the time dimension. More specifically, we compare the

time taken by the unlearned model and the retrained model to reach their respective peak generalization performance. We then report how many times faster our unlearning approach is compared to the retrained baseline.

Appendix E.3 Implementation Details

For the federated learning experiments, we adopt the Adam optimizer with a learning rate of 1×10^{-4} , and each client performs 3 local training epochs per round. Our method is fine-tuned for 40, 30, and 20 rounds after pruning on CIFAR-100, CIFAR-10, and EMNIST, respectively.

Regarding pruning, we set the pruning ratios to 0.3 and 0.4 for CIFAR-10 under IID and Non-IID conditions, respectively, and apply the same ratios for EMNIST. For CIFAR-100, we employ data augmentation techniques to enhance training, which effectively compresses information into the most important neurons while leaving more redundant parameters. Consequently, we adopt higher pruning ratios of 0.8 and 0.85 for CIFAR-100 under IID and Non-IID settings.

Appendix F Ablation Studies

In this section, we examine how the pruning ratio, data distribution, parameter selection, and the number of clients affect the performance of our unlearning algorithms.

Appendix F.1 Effect of Pruning Ratio

In this subsection, we demonstrate how the pruning ratio ρ influences the unlearning performance. As presented in Section 6, the hyperparameter ρ determines how many parameters of the model are re-initialized during unlearning.

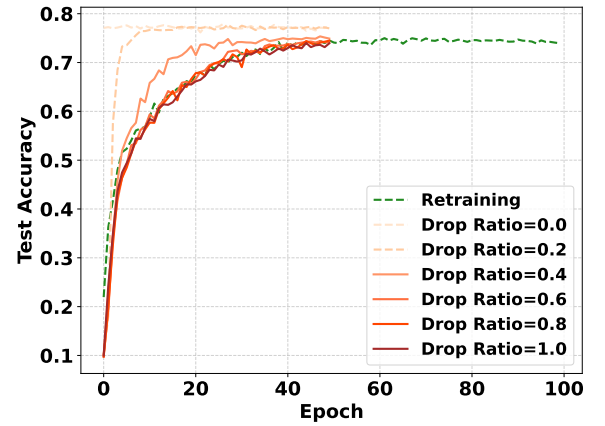


Figure F1: Efficiency comparison across pruning ratios ρ

Table F2 illustrates the performance of the unlearned model under different pruning ratios. When ρ is 0%, it corresponds to pure fine-tuning, which leads to unlearning failure, as no memorization information are removed. In this case, the accuracy gap remains very high, reaching 70.71% on the top memorization group. This indicates that fine-tuning alone is insufficient for unlearning. In

Table F2: Performance of FedMemPrune under different pruning ratios

Pruning Ratio	Accuracy by Unlearning Memorization Score Subgroup (%) ($\Delta \downarrow$)					Unlearning Dataset Acc. (%) ($\Delta \downarrow$)	Test Dataset Acc. (%) \uparrow	Local Fairness (10^{-3}) \downarrow
	Group (95%,100%]	Group (90%,95%]	Group (85%,90%]	Group (80%,85%]	Group (0%,80%]			
0	86.60 \pm 0.22 (70.71)	85.60 \pm 0.59 (54.61)	84.74 \pm 0.88 (46.89)	87.17 \pm 0.59 (36.47)	98.50 \pm 0.21 (9.12)	96.30 \pm 0.10 (15.89)	77.37 \pm 0.22	49.37 \pm 2.09
0.2	43.30 \pm 1.23 (27.41)	49.92 \pm 4.06 (18.93)	56.70 \pm 1.59 (18.85)	68.39 \pm 1.89 (17.69)	94.12 \pm 0.07 (4.74)	87.39 \pm 0.30 (6.98)	77.06 \pm 0.06	31.49 \pm 3.13
0.4	25.55 \pm 2.24 (9.66)	29.42 \pm 1.17 (1.57)	40.65 \pm 1.75 (2.80)	48.36 \pm 2.89 (2.34)	89.00 \pm 0.74 (0.38)	80.72 \pm 0.44 (0.31)	75.36 \pm 0.35	32.55 \pm 6.56
0.6	18.22 \pm 1.53 (2.33)	27.54 \pm 2.72 (3.45)	33.49 \pm 1.54 (4.36)	44.44 \pm 0.59 (6.26)	87.58 \pm 0.54 (1.80)	78.72 \pm 0.31 (1.69)	73.47 \pm 0.51	30.50 \pm 3.46
0.8	19.00 \pm 0.58 (3.11)	25.04 \pm 3.26 (5.95)	35.20 \pm 2.10 (2.65)	46.32 \pm 1.35 (4.38)	88.53 \pm 0.94 (0.85)	79.48 \pm 0.72 (0.93)	74.24 \pm 0.64	40.59 \pm 4.77
1	19.16 \pm 0.66 (3.27)	25.98 \pm 4.03 (5.01)	38.01 \pm 0.88 (0.16)	43.82 \pm 1.55 (6.88)	88.50 \pm 0.62 (0.88)	79.55 \pm 0.34 (0.86)	74.06 \pm 0.82	36.28 \pm 0.90
Retrained Baseline	15.89 \pm 8.80	30.99 \pm 14.61	37.85 \pm 18.07	50.70 \pm 10.43	89.38 \pm 4.27	80.41 \pm 0.09	74.93 \pm 0.32	30.78 \pm 6.58

This table represents the accuracies of the unlearned model Φ_{G_u} on the unlearning dataset D_u , its subgroups $\{T_p\}$ split by memorization scores and test dataset D_{test} , along with the local fairness metric across different pruning ratios. We also denote the difference Δ between the retrained baselines and the corresponding pruning ratio results in blue, and have highlighted the best values in red.

contrast, when ρ equals 40%, meaning that 40% of the parameters are dropped, the unlearned model Φ_{G_u} performs similarly to the retrained model Φ_{G_r} in different subgroups of memorization scores. This suggests that key memorization information in the unlearning dataset D_u have been successfully forgotten, providing evidence for our hypothesis that memorization information are primarily stored in redundant parameters. Moreover, the local fairness reaches 32.55, approaching the retrained baseline that ensures client-level fairness in federated unlearning. In the time dimension, the runtime of the proposed approach represents an improvement 50% over the retrained baseline, as shown in Figure F1.

However, a higher pruning ratio ρ leads to excessive forgetting, resulting in accuracies that are noticeably lower than those of the retrained baseline. Additionally, the unlearning times approaching those of full retraining, as shown in Figure F1. Specifically, when ρ exceeds 60%, the unlearning time closely approaches the retraining time. Therefore, selecting an appropriate pruning ratio ρ is crucial. Nevertheless, the optimal value of ρ depends on the distribution of memorization information across the model parameters, which is influenced by factors such as model architecture, data distribution, and the federated learning setting.

Appendix F.2 Effect of Data Distribution Influence

In this subsection, we examine how data distribution influences federated unlearning. Specifically, we explore how the discrepancy between the remaining dataset and the unlearning dataset impacts the unlearning process.

As discussed in Section 4, the relationship between the remaining dataset and the unlearning dataset is a critical factor in evaluating the difficulty of unlearning. Qualitatively, there are two main scenarios: 1) the remaining dataset and the unlearning dataset exhibit significant overlap, and 2) the two datasets are substantially different. These relationships can be quantitatively described by the degree of the Non-IID data. A higher degree of Non-IID data ($\alpha \downarrow$) implies a smaller overlap between the remaining and unlearning datasets. In an extreme Non-IID scenario ($\alpha \rightarrow 0$), where each client holds data from a single, unique class, unlearning any one client results in minimal overlap. In contrast, IID settings typically

involve more overlapping information, which can result in greater overlap between the two datasets in the context of unlearning.

Table F3 presents the results of our approach under varying degrees of Non-IID distributions using the CIFAR-10 dataset. A Dirichlet distribution is employed to simulate data heterogeneity, where the concentration parameter α controls the degree of Non-IIDness. Overall, our approach performs robustly across different Non-IID scenarios. In the case where $\alpha = 10$, there is significant overlap between the remaining dataset and the unlearning dataset. Under this setting, our method achieves performance comparable to the retrained baseline across all memorization score groups. Specifically, the accuracy of the entire unlearning dataset on the unlearned model using our method reaches 77.99%, closely matching the retrained baseline at 77.76%. Moreover, our method ensures fairness comparable to retrained baselines. However, the fine-tuning approach fails to unlearn any information, maintaining nearly 100% accuracy across all memorization score subgroups. This suggests that fine-tuning alone is insufficient to remove significantly overlapping information. On the other hand, when $\alpha \rightarrow 0$, indicating no overlap between clients' data, fine-tuning alone can achieve optimal unlearning performance. This observation is consistent with the principle of catastrophic forgetting [13], where fine-tuning only on the remaining dataset may naturally cause the model to forget information associated with the unlearning dataset if there is no information overlap between them.

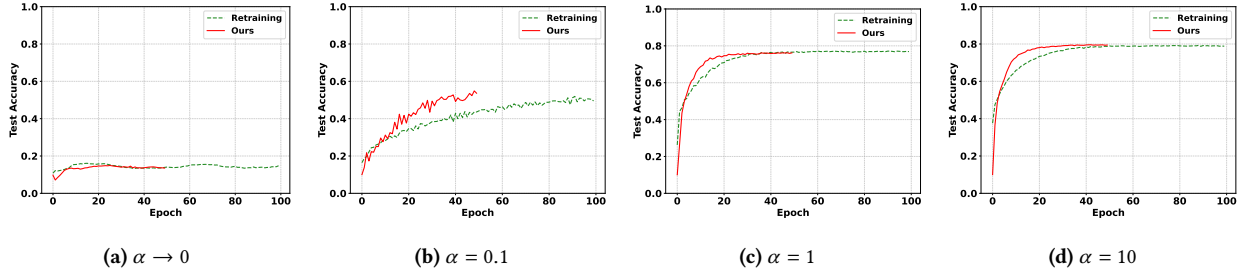
Due to the unlearning failure of the only fine-tuning approach, we conduct the time analysis exclusively on our method. Figure F2 illustrates the comparison of test performance over time between our method and the retrained baseline. In cases where $\alpha \rightarrow 0$ and $\alpha = 0.1$, representing extreme Non-IID scenarios, the behavior is relatively unstable. For more general distributions, our method achieves approximately a 50% improvement in time efficiency compared to the retrained baseline. This demonstrates that our method is time-efficient across various distribution scenarios.

As α approaches 0, the data distribution becomes increasingly Non-IID. From the results, we observe that in the extreme Non-IID setting (i.e., $\alpha \rightarrow 0$), fine-tuning alone can effectively achieve unlearning. However, as the Non-IID degree decreases, the effectiveness of fine-tuning for unlearning diminishes. For instance, when $\alpha = 10$, fine-tuning fails to remove the unlearning dataset, as indicated by the high accuracy across all memorization score groups

Table F3: Performance of FedMemPrune across different Non-IID scenarios

Non-IID Degree	Accuracy by Unlearning Memorization Score Subgroup (%) ($\Delta \downarrow$)					Unlearning Dataset Acc. (%) ($\Delta \downarrow$)	Test Dataset Acc. (%) \uparrow	Local Fairness (10^{-3}) \downarrow
	Group (95%,100%]	Group (90%,95%]	Group (85%,90%]	Group (80%,85%]	Group (0%,80%]			
$\alpha \rightarrow 0$								
Only Fine-tuning	0.00 \pm 0.00 (0.00)	0.00 \pm 0.00 (0.00)	0.00 \pm 0.00 (0.00)	0.00 \pm 0.00 (0.00)	0.00 \pm 0.00 (0.00)	0.00 \pm 0.00 (0.00)	16.26 \pm 1.42	63.12 \pm 3.71
Ours	0.00 \pm 0.00 (0.00)	0.00 \pm 0.00 (0.00)	0.00 \pm 0.00 (0.00)	0.00 \pm 0.00 (0.00)	0.00 \pm 0.00 (0.00)	0.00 \pm 0.00 (0.00)	12.87 \pm 1.39	67.70 \pm 11.78
Retrained Baseline	0.00 \pm 0.00	0.00 \pm 0.00	0.00 \pm 0.00	0.00 \pm 0.00	0.00 \pm 0.00	0.00 \pm 0.00	13.92 \pm 0.70	98.57 \pm 13.90
$\alpha = 0.1$								
Only Fine-tuning	92.79 \pm 1.46 (44.40)	89.79 \pm 0.80 (36.56)	80.75 \pm 1.50 (30.49)	85.53 \pm 0.97 (31.14)	52.44 \pm 1.55 (13.40)	56.41 \pm 1.33 (15.11)	54.54 \pm 0.16	126.43 \pm 2.51
Ours	51.35 \pm 6.21 (2.96)	54.26 \pm 6.63 (1.03)	50.78 \pm 7.40 (0.52)	49.61 \pm 7.99 (4.78)	37.88 \pm 2.50 (1.16)	40.12 \pm 3.01 (1.18)	50.26 \pm 2.44	267.25 \pm 124.71
Retrained Baseline	48.39 \pm 17.43	53.23 \pm 16.03	50.26 \pm 11.31	54.39 \pm 6.36	39.04 \pm 1.45	41.30 \pm 2.77	51.34 \pm 1.35	110.65 \pm 45.80
$\alpha = 1$								
Only Fine-tuning	100.00 \pm 0.00 (84.93)	99.62 \pm 0.00 (83.47)	98.98 \pm 0.18 (72.93)	95.51 \pm 0.48 (68.84)	97.63 \pm 0.11 (13.36)	97.73 \pm 0.10 (23.54)	76.73 \pm 0.12	10.35 \pm 0.02
Ours	25.67 \pm 2.71 (10.60)	25.51 \pm 1.45 (9.36)	34.10 \pm 0.54 (8.05)	37.82 \pm 3.44 (11.15)	80.96 \pm 0.35 (3.31)	73.26 \pm 0.33 (0.93)	76.38 \pm 0.25	9.16 \pm 0.07
Retrained Baseline	15.07 \pm 10.66	16.15 \pm 11.42	26.05 \pm 18.42	26.67 \pm 18.86	84.27 \pm 3.14	74.19 \pm 0.55	77.46 \pm 0.42	3.70 \pm 0.58
$\alpha = 10$								
Only Fine-tuning	100.00 \pm 0.00 (93.00)	99.85 \pm 0.22 (86.76)	99.54 \pm 0.00 (80.36)	98.63 \pm 0.00 (66.67)	99.63 \pm 0.01 (7.05)	99.60 \pm 0.01 (21.84)	78.69 \pm 0.02	1.45 \pm 0.00
Ours	14.16 \pm 1.63 (7.16)	22.68 \pm 2.28 (9.59)	33.33 \pm 3.19 (14.15)	48.71 \pm 3.58 (16.75)	89.84 \pm 1.48 (2.74)	77.99 \pm 1.49 (0.23)	77.87 \pm 1.32	2.96 \pm 0.87
Retrained Baseline	7.00 \pm 4.96	13.09 \pm 9.29	19.18 \pm 13.61	31.96 \pm 21.13	92.58 \pm 3.36	77.76 \pm 0.63	78.59 \pm 0.38	5.57 \pm 7.04

This table shows the accuracies of the unlearned model Φ_{G_u} on the unlearning dataset D_u , its subgroups $\{T_p\}$ split by memorization scores and test dataset D_{test} , along with the local fairness metric across different Non-IID scenarios.

**Figure F2: Efficiency comparison between unlearning and retraining for different Non-IID scenarios.**

(e.g., 100.00%, 100.00%, 100.00%, 99.09%, 98.63%, 99.69%). This suggests that when the unlearning dataset and the remaining dataset have no overlap, fine-tuning alone can effectively perform unlearning. Additionally, another key observation is that fine-tuning mainly updates overlapping information, while memorization information are harder to forget. This is evident in cases like $\alpha = 0.1$, where the accuracy of the highest memorization group (e.g., 88.42%) remains significantly higher than that of the lowest memorization group (e.g., 48.08%). This finding supports our claim that memorization information are primarily stored in redundant parameters rather than in the critical ones.

Appendix F.3 Important or Redundant Parameters Selection

In this section, we compare different parameter selection methods. There are several existing machine unlearning methods based on the removal of important parameters, in contrast to our approach, which focuses on the removal of redundant parameters. Important parameters are defined as those that contribute significantly to

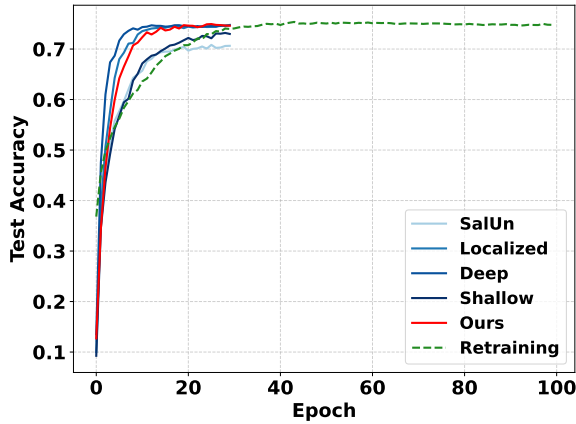
learning, typically characterized by large gradients or large weights. These methods aim to remove important parameters associated with the unlearning dataset D_u and require access to D_u during the unlearning process. Although the unlearning dataset D_u is not accessible during the unlearning stage in our setting, and these methods are originally designed as machine unlearning algorithms that may not be suitable for federated learning systems, we relax these requirements and adopt these parameter selection methods as comparative baselines. The methods we select included:

- **SalUn** [8]. The **SalUn Selection** selects parameters with the highest gradient magnitudes, based on the principles of saliency maps.
- **Localized Strategy Selection** [43]. The **Localized Strategy Selection** is a recently proposed parameter selection method that chooses channel-wise neurons with the highest magnitude of the weighted gradient (i.e., the product of parameters and gradients).
- **Deep Layers**. The **Deep Layers Selection** is motivated by previous studies on the structural localization of unlearning

Table F4: Performance comparison of FedMemPrune vs. baselines with different selection strategies

Parameter Selection	Accuracy by Unlearning Memorization Score Subgroup (%) ($\Delta \downarrow$)					Unlearning Dataset Acc. (%) ($\Delta \downarrow$)	Test Dataset Acc. (%) \uparrow	Local Fairness (10^{-3}) \downarrow
	Group (95%,100%]	Group (90%,95%]	Group (85%,90%]	Group (80%,85%]	Group (0%,80%]			
SalUn	15.20 \pm 1.18 (2.40)	41.33 \pm 1.24 (6.93)	60.00 \pm 0.57 (17.60)	75.60 \pm 1.13 (16.53)	95.15 \pm 0.92 (3.97)	86.40 \pm 0.63 (3.91)	70.29 \pm 0.27	0.35 \pm 0.06
Localized	23.60 \pm 3.71 (10.80)	52.00 \pm 1.82 (17.60)	74.13 \pm 1.54 (3.47)	86.27 \pm 2.36 (5.86)	98.40 \pm 0.12 (0.72)	90.79 \pm 0.23 (0.48)	74.40 \pm 0.30	0.32 \pm 0.03
Deep	26.80 \pm 0.57 (14.00)	57.33 \pm 2.07 (22.93)	78.53 \pm 0.38 (0.93)	88.93 \pm 1.80 (3.20)	98.79 \pm 0.17 (0.33)	91.84 \pm 0.19 (1.53)	74.65 \pm 0.23	0.13 \pm 0.02
Shallow	18.80 \pm 3.31 (6.00)	44.00 \pm 1.42 (9.60)	65.87 \pm 0.50 (11.73)	78.00 \pm 3.31 (14.13)	95.61 \pm 0.12 (3.51)	87.48 \pm 0.22 (2.83)	72.87 \pm 0.45	0.54 \pm 0.08
Ours	20.93 \pm 1.80 (8.13)	49.73 \pm 1.68 (15.33)	68.00 \pm 1.82 (9.60)	84.67 \pm 1.24 (7.46)	96.96 \pm 0.85 (2.16)	89.36 \pm 0.67 (0.95)	73.67 \pm 0.72	0.50 \pm 0.05
Retrained Baseline	12.80 \pm 9.34	34.40 \pm 19.80	77.60 \pm 14.71	92.13 \pm 5.58	99.12 \pm 0.62	90.31 \pm 0.16	74.79 \pm 0.38	0.01 \pm 0.00

This table demonstrates the accuracies of the unlearned model Φ_{G_u} on the unlearning dataset D_u , its subgroups $\{T_p\}$ split by memorization scores and test dataset D_{test} , along with the local fairness metric across different parameter selection methods.

**Figure F3: Efficiency comparison across different parameter selection methods**

information in neural networks [32]. This method adopts the selection strategy of **SalUn** [8] but restricts the selection to deep layers.

- **Shallow Layers.** The **Shallow Layers Selection** follows the same selection method as **Deep Layers Selection**, but focuses on selecting parameters from shallow layers.

(*Noted. we only apply the parameter selection strategies of these methods, not their completed frameworks.*)

We conduct the experiment under the CIFAR-10 IID setting and attempt to unlearn one client out of ten clients. The results of the unlearning process are summarized in Table F4. These outcomes highlight the trade-offs between different parameter selection strategies and their effects on both generalization and unlearning performance across various memorization score subgroups.

Firstly, we observe that the results are relatively similar across different parameter selection strategies. Specifically, the **SalUn Selection** approach, which ranks parameters by saliency, results in significant drops in accuracy across all memorization score subgroups, particularly in the high-score ranges. A similar trend is observed in the **Shallow Layers Selection** strategy. This suggests that these methods tend to remove parameters that are crucial for representing the unlearning dataset D_u , often leading to excessive

forgetting and degradation in performance on both the unlearning dataset and the test dataset. For the entire unlearning dataset, the accuracies drop to 86.40% and 87.48%, compared to 90.31% for the re-trained model, indicating excessive forgetting. Moreover, the test accuracies decrease to 70.29% and 72.87%, respectively, in comparison to the baseline accuracy of 74.79%, implying reduced generalization performance. In contrast, the **Localized Strategy Selection** and **Deep Layers Selection** strategies preserve some memorization information, as evidenced by the higher accuracies in the top memorization score group: 23.60% and 26.80%, respectively, compared to the baseline of 12.80%.

These findings suggest that important parameters for the unlearning dataset mainly encode overlapping and general information. Removing these parameters may disable some memorization and overlapping representations, while overlapping information may be recovered through fine-tuning on the remaining dataset D_r . That is feasible, but our proposed method demonstrates greater precision. Unlike **SalUn Selection** and **Shallow Layers Selection**, which tend to forget excessive information, and unlike **Localized Strategy Selection** and **Deep Layers Selection**, which retain some memorization information, our method maintains a moderate and balanced effect across all memorization score subgroups. It specifically targets parameters associated with memorization. Further discussion on the relationship between parameters and information is provided in Appendix H.1. For local fairness, all selection strategies demonstrate comparable performance.

Regarding time efficiency, the observed trends are expected. As shown in Figure F3, our method also demonstrates moderate run-time performance. The **SalUn Selection** and **Shallow Layers Selection** strategies are more difficult to fine-tune due to excessive forgetting. Conversely, the **Localized Strategy Selection** and **Deep Layers Selection** approaches retain some memorization information, enabling quicker performance recovery.

In summary, our parameter selection method is both moderate and precise, making it particularly suitable for federated unlearning scenarios where the unlearning dataset D_u is unavailable during the unlearning phase.

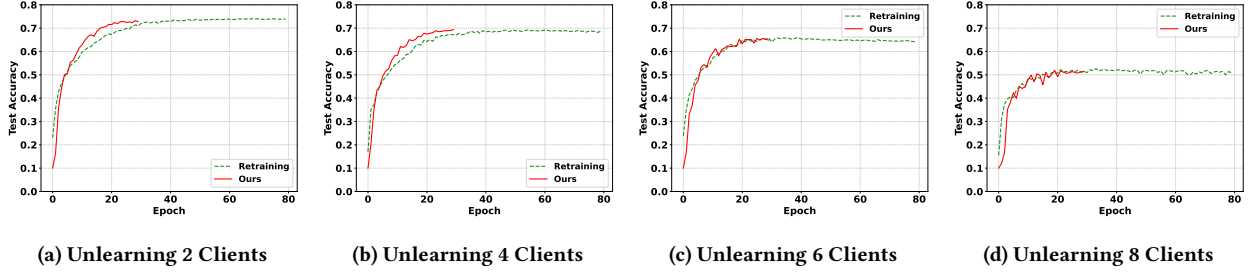
Appendix F.4 Unlearning Multiple Clients

In this subsection, we evaluate the effectiveness of our method in a multi-client unlearning setting. Specifically, we simulate the removal of 2, 4, 6, and 8 clients from a federated learning system

Table F5: Performance of FedMemPrune under multiple clients unlearning scenarios

Client	Accuracy by Unlearning Memorization Score Subgroup (%) ($\Delta \downarrow$)					Unlearning Dataset Acc. (%) ($\Delta \downarrow$)	Test Dataset Acc. (%) \uparrow	Local Fairness (10^{-3}) \downarrow
	Group (95%,100%]	Group (90%,95%]	Group (85%,90%]	Group (80%,85%]	Group (0%,80%]			
2 Clients ($\rho = 0.4$)								
Ours	18.44 \pm 1.71 (6.56)	25.06 \pm 0.95 (5.96)	34.26 \pm 1.16 (12.14)	40.68 \pm 0.95 (10.13)	87.11 \pm 0.16 (3.06)	76.89 \pm 0.17 (0.52)	73.17 \pm 0.31	88.80 \pm 5.52
Retrained Baseline	11.88 \pm 8.44	19.10 \pm 13.53	22.12 \pm 15.51	30.55 \pm 13.82	90.17 \pm 4.13	77.41 \pm 0.77	73.90 \pm 0.69	68.54 \pm 14.64
4 Clients ($\rho = 0.4$)								
Ours	19.99 \pm 1.61 (7.47)	27.14 \pm 1.99 (9.32)	30.17 \pm 1.57 (10.57)	33.40 \pm 2.17 (9.79)	76.22 \pm 1.69 (3.65)	68.65 \pm 1.59 (1.22)	68.79 \pm 1.09	87.88 \pm 4.86
Retrained Baseline	12.52 \pm 8.93	17.82 \pm 12.62	19.60 \pm 13.89	23.61 \pm 16.70	79.87 \pm 2.41	69.87 \pm 0.44	68.78 \pm 0.30	82.42 \pm 10.46
6 Clients ($\rho = 0.5$)								
Ours	18.22 \pm 1.01 (5.95)	22.25 \pm 1.43 (8.22)	24.05 \pm 1.23 (8.45)	27.11 \pm 1.79 (9.21)	67.54 \pm 0.29 (1.49)	62.65 \pm 0.31 (0.02)	64.62 \pm 0.35	52.73 \pm 8.26
Retrained Baseline	12.27 \pm 8.69	14.03 \pm 9.93	15.60 \pm 11.03	17.90 \pm 12.70	69.03 \pm 2.79	62.63 \pm 0.50	64.06 \pm 0.28	70.37 \pm 17.79
8 Clients ($\rho = 0.6$)								
Ours	13.10 \pm 1.06 (6.96)	16.00 \pm 1.41 (6.52)	18.76 \pm 1.11 (8.43)	21.37 \pm 0.70 (9.00)	49.21 \pm 0.92 (0.61)	48.83 \pm 0.81 (0.66)	51.87 \pm 0.57	417.23 \pm 17.96
Retrained Baseline	6.14 \pm 4.36	9.48 \pm 6.75	10.33 \pm 7.34	12.37 \pm 8.75	49.82 \pm 2.33	48.17 \pm 1.44	50.86 \pm 1.43	119.65 \pm 26.38

This table shows the accuracies of the unlearned model Φ_{G_u} on the unlearning dataset D_u , its subgroups $\{T_p\}$ split by memorization scores and test dataset D_{test} , along with the local fairness metric across multiple clients unlearning scenarios.

**Figure F4: Efficiency comparison between unlearning and retraining for multiple clients.**

comprising 10 clients under a CIFAR-10 Non-IID partitioning. Table F5 presents the accuracy of the unlearned model Φ_{G_u} across memorization-based subgroups of the unlearning dataset D_u , as well as the overall performance on D_u and the general test set D_{test} . It also provides the evaluation of local fairness.

The results demonstrate that our method consistently achieves effective unlearning across all configurations. Compared to the retrained baseline, our approach produces similar subgroup accuracies, while maintaining competitive or superior performance on the test dataset. For instance, when unlearning 8 clients, our method achieves a substantial reduction in high memorization group accuracies (e.g., 13.10% vs. 6.14% in the [95%, 100%] group), and still retains a test accuracy of 51.87%. This trend is consistent in all unlearning cases: our approach consistently achieves similar accuracies on memorization-based subgroups while maintaining meaningful accuracy on the test dataset. Moreover, this proves that our method can even prune synergic information through we cannot directly evaluate this. Furthermore, in local fairness evaluation, our approach maintains fairness levels that are largely consistent with the retrained baselines, except in the case of unlearning 8 out of 10 clients. In this extreme setting, removing too much learned knowledge may introduce uncontrolled randomness.

Considering time consumption, Figure F4 illustrates a clear efficiency advantage of our method over the retraining baselines

when unlearning a small proportion of clients (i.e., fewer than 50%). However, when unlearning the majority of the knowledge from the federated learning system, the important overlapping information and synergic information learned from the entire dataset D are disrupted. Consequently, essential patterns are removed, causing the model to degrade toward the random state. As a result, the fine-tuning process begins to resemble full retraining, particularly when unlearning 8 out of 10 clients. This phenomenon underscores an extreme scenario where removing common patterns, instead of specific memorization information, can disable the model and make the unlearning become retraining.

Appendix F.5 Effect of Client Number

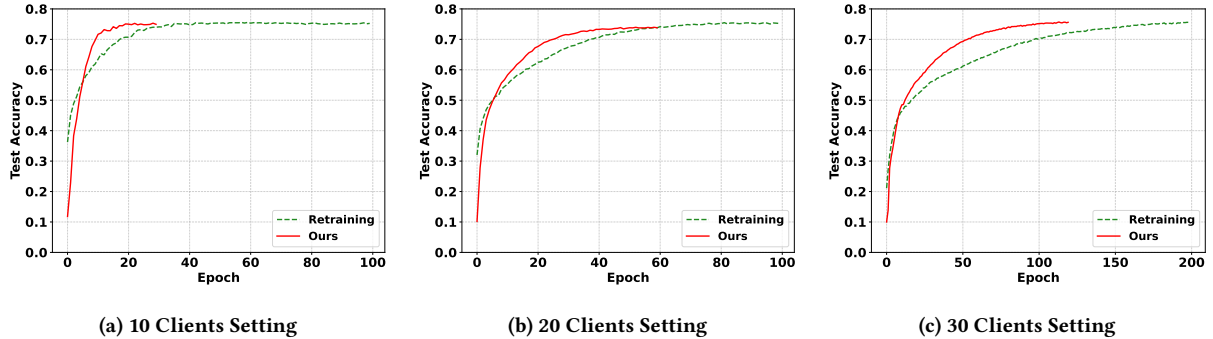
In this subsection, we examine how large-scale federated learning (FL) settings impact our algorithm. In principle, our approach targets the removal of redundant parameters; therefore, increasing the number of clients in an FL configuration is not expected to significantly influence the performance of our unlearning algorithm.

Table F6 presents the performance of our unlearned model under various large-scale FL settings. Specifically, our method achieves performance gaps of 7.47%, 3.20%, and 8.00% on the top memorized subgroup compared to the retrained baselines for configurations

Table F6: Performance of FedMemPrune under various large-scale FL settings

Client	Accuracy by Unlearning Memorization Score Subgroup (%) ($\Delta \downarrow$)					Unlearning Dataset Acc. (%) ($\Delta \downarrow$)	Test Dataset Acc. (%) \uparrow	Local Fairness (10^{-3}) \downarrow
	Group (95%,100%]	Group (90%,95%]	Group (85%,90%]	Group (80%,85%]	Group (0%,80%]			
10 Clients								
Ours	20.27 ± 1.54 (7.47)	50.40 ± 3.44 (16.00)	70.93 ± 2.29 (6.67)	85.60 ± 0.86 (6.53)	98.66 ± 0.20 (0.46)	90.56 ± 0.35 (0.25)	74.97 ± 0.27	0.91 ± 0.06
Retrained Baseline	12.80 ± 9.34	34.40 ± 19.80	77.60 ± 14.71	92.13 ± 5.58	99.12 ± 0.62	90.31 ± 0.16	74.79 ± 0.38	0.14 ± 0.01
20 Clients								
Ours	41.87 ± 1.36 (3.20)	54.13 ± 1.51 (6.13)	64.80 ± 0.65 (5.60)	71.20 ± 1.13 (2.13)	95.01 ± 0.11 (1.56)	87.56 ± 0.23 (1.25)	73.56 ± 0.18	5.22 ± 0.08
Retrained Baseline	38.67 ± 7.64	48.00 ± 12.26	70.40 ± 9.13	73.33 ± 2.38	96.57 ± 0.04	88.81 ± 0.30	74.51 ± 0.21	6.54 ± 0.26
50 Clients								
Ours	58.00 ± 3.27 (8.00)	60.67 ± 1.89 (1.34)	62.67 ± 0.94 (7.33)	74.00 ± 1.63 (1.33)	91.00 ± 0.28 (0.37)	85.00 ± 0.33 (0.40)	75.61 ± 0.13	7.78 ± 0.65
Retrained Baseline	50.00 ± 8.83	59.33 ± 10.94	70.00 ± 4.63	72.67 ± 3.94	90.63 ± 0.10	84.60 ± 0.24	74.88 ± 0.11	9.34 ± 0.19

This table shows the accuracies of the unlearned model Φ_{G_u} on the unlearning dataset D_u , its subgroups $\{T_p\}$ split by memorization scores and test dataset D_{test} , along with the local fairness metric across different large-scale FL unlearning scenarios.

**Figure F5: Efficiency comparison between unlearning and retraining under various large-scale FL settings.**

with 10, 20, and 50 clients, respectively. Furthermore, the generalization and fairness of the unlearned models remain comparable to those of the retrained baselines across all settings. Figure F5 illustrates the time efficiency of our unlearning algorithm. Notably, FedMemPrune maintains its computational efficiency under different large-scale FL settings.

Appendix G Revisiting Existing Federated Unlearning Evaluation Metrics

In this section, we will revisit the unlearning evaluation metrics through the lens of memorization. Federated unlearning algorithms could be evaluated through multiple metrics. However, from the perspective of memorization, some of these metrics are unrealistic, certain metrics prove to be impractical, as they cannot definitively confirm that the influence of the unlearning data has been completely removed. Within the context of the unlearning problem, retraining is the gold standard, which basically means that all unlearned models are expected to approach the retrained model. Therefore, in this section, we mainly employ retrained models to analyze these metrics and initially investigate the tasks that clients identify as unlearning targets.

Appendix G.1 Revisiting Metrics based on Parameter Differences

The parameter difference assesses the differences between the unlearned model and the retrained model within the parameter space. If the unlearned model becomes more similar to the retrained model, it indicates a successful unlearning result. The common parameter difference metrics include $L2$ distance [36, 46], *Kullback–Leibler divergence* [11, 46] and *cosine similarity* [28, 29].

However, these metrics do not consider the relationship between the unlearning data and the remaining data. If the unlearning dataset is closely similar to the remaining dataset, the difference in parameters between the unlearned model and the original model may become insignificant. Additionally, this metric does not account for the stochastic nature of retraining. Models retrained on the same remaining dataset can still reach different local optimal points. We conducted an easy experiment to demonstrate our findings.

Experiment. In this experiment, we mainly utilize *Cifar-10* [25] as the dataset and *Resnet18* [19] as the network architecture. Subsequently, we construct an FL framework involving 10 clients and simulate the process of unlearning one of them. Specifically, we begin by training an original model using all 10 clients, and to simulate the unlearning process, we exclude the client who requests unlearning and proceed to retrain several unlearned models with the remaining 9 clients. Here all unlearned models are retrained on

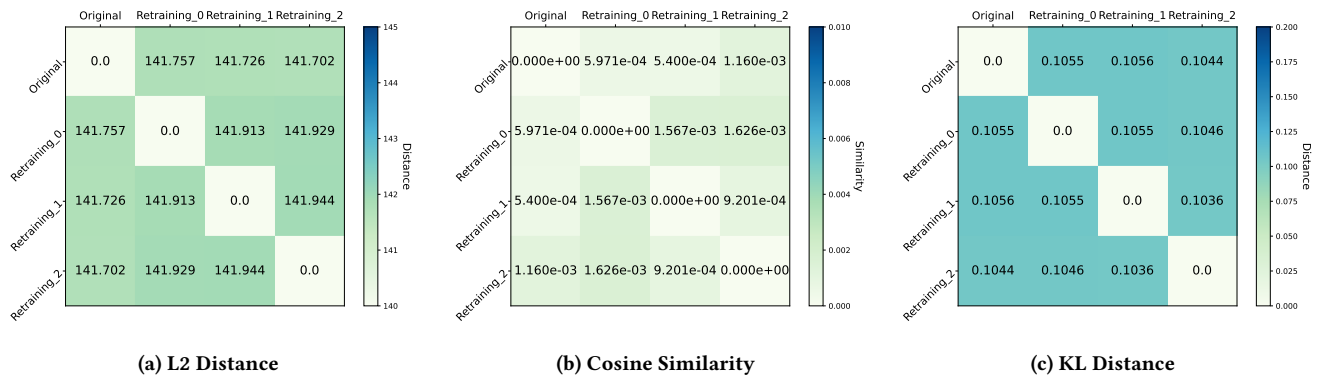


Figure G6: Parameter differences measurement between models.

the remaining clients. Finally, we will employ different parameter difference metrics on these models to support our viewpoint with evidence.

Table G7: Accuracies of original and retrained models

Models	Training Dataset Acc.(%)	Test Dataset Acc.(%)	Unlearning Dataset Acc.(%)
Original Model	95.01	76.08	99.37
Retrained Model No.0	95.60	73.96	79.06
Retrained Model No.1	95.81	74.52	80.28
Retrained Model No.2	96.02	75.31	80.49

Findings. The performance of the models is presented in Table G7. In general, all models have successfully converged. In addition, retrained models show similar performance in the test dataset, achieving approximately 74% precision. Their performance in the unlearning dataset is also consistent, with accuracies around 80%.

In Figure G6, we illustrate three distinct distance metrics. The 'Original' refers to the model trained using the unlearning dataset, whereas the 'Retraining' refers to the models trained excluding the unlearning dataset. We create one original model and three retrained models, and then assess the distances among them. We have the following findings:

- **There exists the significant distance between the retrained models.** In Figure G6a, It has been noted that the L2 distances among the retrained models are all close to 141. Additionally, in Figure G6b, the cosine similarities between retrained models approaches 0. This suggests that these retrained models do not exhibit similarity in parameter space.
- **The distance between the retrained models is not significant compared to the original model.** For example, in Figure G6a, the L2 distance between the retrained model no.0 and the original model is 141.757, however, the distance between the retrained model no.0 and no.1 is 141.913, which is not significant. If apply the KL distance, the distances of retrained model no.0 to retrained model no.1 and the original model are both around 0.1055, which shown in

the Figure G6c. Therefore, when considering the retrained models, their distance proves to be relatively insignificant in comparison to the original model.

Basically, our experiments demonstrate that unlearned models may not approach the retrained models in the parameter space. In fact, even retrained models themselves can differ significantly from one another, highlighting the stochastic nature of training. While the unlearned model may successfully forget the unlearned dataset, it may still differ from the baseline retrained model. Additionally, if the unlearning dataset shares a similar feature distribution with the remaining data, this can lead to indistinguishability between the unlearned model and the original model in the parameter space. Overall, metrics based on parameter distance are not effective for evaluating unlearning.

Appendix G.2 Revisiting Metrics based on Performance Metrics

Performance metrics like accuracy or loss of the unlearning dataset are commonly employed in the unlearning task to directly assess the unlearning results. Nonetheless, these metrics for the unlearning dataset overlook the distinctions between each unlearning example. The close accuracy or loss of the unlearning dataset, when compared to the retrained model performance, cannot guarantee the unlearning effect for each example. In the extreme case, some unlearning algorithms may primarily unlearn generalized examples in the unlearning dataset, resulting in similar accuracy compared to the retrained model, but this does not remove the impact of memorization information. Furthermore, retrained models might memorize examples randomly, resulting in a significant variation in how they perform on particular examples within the unlearning dataset. This makes it difficult for a single retrained model to serve as a reliable baseline. Our experiment would show our findings.

Experiment. In this experiment, we also utilize Cifar-10 [25] as the dataset and Resnet18 [19] as the network architecture. Subsequently, we still construct an FL framework involving 10 clients and simulate the process of unlearning one of them. Here, we directly retrain multiple global models with the remaining 9 clients. Then we can compare the example-level performance with these retrained models.

Findings. We evaluate the classification probability of each example within the unlearning dataset in multiple retrained models. We illustrate the results in Figure G7. It shows the correct classification probability of each example in the unlearning dataset on the different retrained models and these examples are sorted by the average correct classification probability. We can find:

- **Majority of examples are classified absolutely correctly.** Obviously, a substantial portion of the examples (examples with indices starting at 2000) are classified correctly even if these examples are not in the remaining dataset. This suggests that there is an overlap between the unlearning dataset and the remaining dataset. It indicates that the overlapping information will not be forgotten even using retraining.
- **A portion of examples have unstable performance.** Notably, there exists a portion of examples with varying classification probabilities on different retrained models. This variability implies that some examples are more sensitive to the stochastic retraining process.

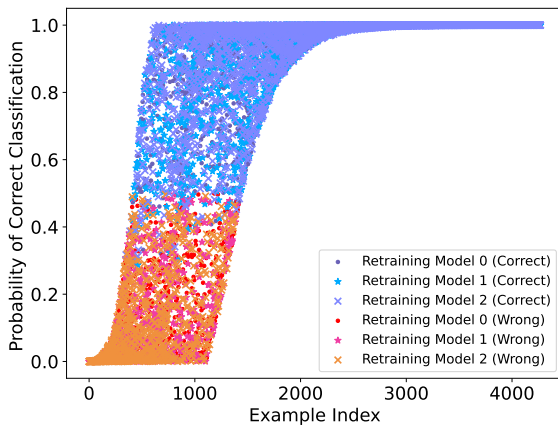


Figure G7: Classification probability of unlearning examples in retrained models.

Based on these findings, traditional performance metrics, such as accuracy or loss in the unlearning dataset, can be misleading. They fail to capture example-level differences that are critical to understanding whether individual data points have been effectively forgotten. Additionally, we notice that some examples exhibit unstable performance. This variability in classification probabilities is driven by rare or under-represented features in the remaining dataset [9]. During retraining, models may randomly memorize the information, resulting in inconsistent performance on these unstable examples. Therefore, performance metrics are not enough to measure unlearning, especially at the example-level.

Appendix G.3 Revisiting Backdoor Evaluation

In the context of unlearning, a backdoor evaluation is a typical assessment used to explicitly show the outcomes of the unlearning

effect. In backdoor attacks, a backdoor trigger is injected into a portion of training data, and those are re-labeled to a pre-defined class. After the normal training, the original model will learn backdoor features. Therefore, in the subsequent unlearning step, if the backdoor features have been completely unlearned, the unlearning algorithm can be considered successful. Currently, this evaluation has widely used in many works [16, 27, 34, 53].

Nevertheless, it is observed that a fundamental issue in backdoor evaluation is that backdoor features are typically irrelevant to the unlearning dataset. In our Definition 3, when utilizing backdoor evaluation, it suggests that the backdoor features are purely memorization information and do not overlap with the remaining information. An unlearning algorithm being able to unlearn the unlearning dataset consisting of all backdoor features does not imply that it can also unlearn a dataset that includes intersections with the remaining information. We also conducted an experiment to support our opinion.

Experiment. In this experiment, we still utilize Cifar-10 [25] as the dataset and Resnet18 [19] as the network architecture. Subsequently, we still construct an FL framework involving 10 clients and simulate the process of unlearning one of them. To conduct the backdoor evaluation, we train two original models: one with the standard unlearning dataset and the other with the backdoor unlearning dataset. After this, we proceed by fine-tuning the two original models with the remaining clients to mimic the unlearning process and then evaluating the fine-tuned models' performance on the unlearning datasets.

Findings. We compare the performance of backdoor training and normal training in Figure G8. The figure G8a shows the trend in test accuracy (solid line) and accuracy on the unlearning dataset (dotted line) at the normal training stage with the unlearning dataset (blue background) and the fine-tuning stage without the unlearning dataset (red background). The figure G8b is similar, but the unlearning dataset is the backdoor dataset. Comparing the two sub-figures, we can observe:

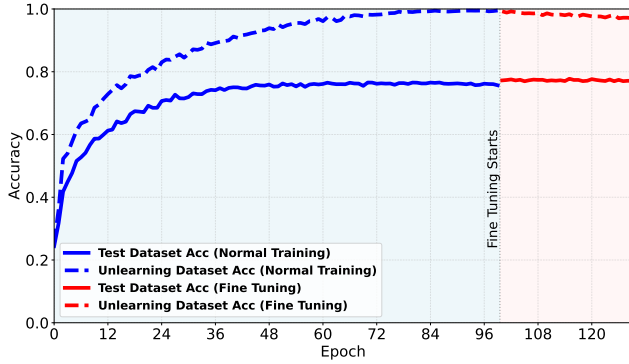
- **For normal training, fine-tuning may not remove the influence of the unlearning dataset.** A slight decrease in the accuracy of the unlearning dataset is observed at the fine-tuning stage.
- **Fine-tuning on the remaining dataset can easily unlearn the backdoor dataset.** Backdoor dataset will be forgot quickly in the fine-tuning stage.

Obviously, backdoor evaluation overlooks the relationship between the unlearning dataset and the remaining dataset. The unlearning dataset may share general information with the remaining data, making it challenging to achieve effective unlearning through fine-tuning. In contrast, backdoor datasets typically contain conflicting information relative to the remaining dataset, which can facilitate unlearning during the fine-tuning process. Therefore, in the evaluation of unlearning algorithms, successful unlearning of a backdoor dataset does not necessarily indicate the overall effectiveness of the algorithm.

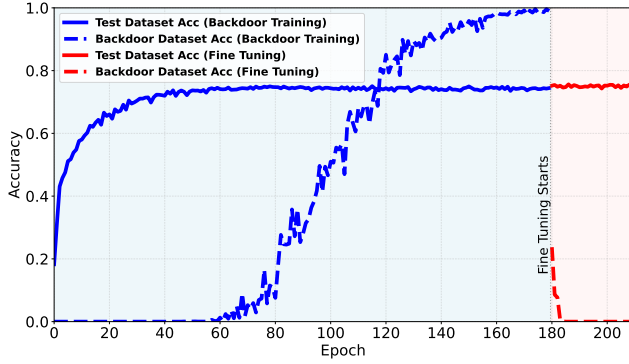
Table H8: Unlearning performance comparison across different reset strategy

Memorization Score Subgroups	Accuracy by Selection Strategy (%)	
	Important Parameters	Redundant Parameters
Group (90%,100%]	19.00	29.60
Group (80%,90%]	24.60	42.00
Group (70%,80%]	23.60	42.20
Group (60%,70%]	24.80	49.60
Group (0%,60%]	28.52	52.37

This table presents the accuracies of the unlearned model Φ_{G_u} on the memorization subgroups $\{T_{p'}\}$ of the unlearning dataset D_u , with different parameter selection strategies applied during unlearning under the CIFAR-10 IID condition.



(a) Normal training and fine tuning



(b) Backdoor training and fine tuning

Figure G8: Backdoor vs normal training performance comparison in the fine-tuning stage.

Appendix H Discussion

Appendix H.1 Parameters and Information Representation

In this subsection, we investigate the relationship between model parameters and learned information.

Currently, the interpretability of neural networks and the way parameters encode information remain open research questions. Consequently, our analysis primarily provides a qualitative investigation of parameter resetting in the context of unlearning memorization information from the unlearning dataset.

According to prior interpretability studies based on saliency maps [39] and activations [35], parameters exhibiting large gradients or large weighted gradients are typically considered important, as they are likely to encode information that mainly contributes to generalization performance. In contrast, other parameters are often unimportant or redundant and may correspond to memorization information. In the context of federated unlearning, we consider two main parameter selection strategies as discussed earlier: 1) resetting important parameters with respect to the unlearning dataset; and 2) resetting redundant parameters with respect to the remaining dataset.

For the first strategy, resetting the important parameters associated with the unlearning dataset followed by fine-tuning on the remaining dataset can achieve unlearning, as shown in Appendix F.3. This works because the fine-tuning stage helps the model to relearn overlapping information while naturally forgetting some memorization information. This forgetting phenomenon resembles catastrophic forgetting [13], as it results from the domain shift between the unlearning dataset and the remaining dataset. As a result, in this fine-tuning stage, the model can forget some previous learned particular or memorization information. However, if the important parameters are not reset, fine-tuning alone may induce only minimal forgetting, and the process of unlearning might not succeed because gradient updates mainly maintain generalization performance.

The second strategy focuses on resetting redundant parameters, which is often more appropriate. As discussed in Appendix F.3, the first strategy might inadvertently retain some memorization information or erase too many general or overlapping patterns, since unlearning is primarily driven by natural forgetting during fine-tuning. In contrast, the second strategy explicitly targets redundant parameters that encode memorization information, offering a more precise unlearning mechanism. Fine-tuning subsequently enhances the forgetting effect further.

To empirically demonstrate the impact of parameter removal on different information types without fine-tuning, we conducted a simple experiment under the CIFAR-10 IID setting. Specifically, we reset approximately 5% of the model parameters using both selection strategies. Table H8 compares the resulting accuracies across various memorization subgroups of the unlearning dataset. We observe that resetting important parameters degrades accuracy across all memorization subgroups, with scores of 19.00%, 24.60%, 23.60%, 24.80%, and 28.52%, respectively. In contrast, resetting redundant parameters significantly reduces performance on the most memorized subgroup (to 29.60%) while preserving performance on less memorized subgroups (e.g., up to 52.37%). These results support the hypothesis that important parameters primarily encode overlapping information, whereas redundant parameters are more closely tied to memorization information. At the example level, memorization examples rely on memorization information and overlapping information, whereas generalized examples in the

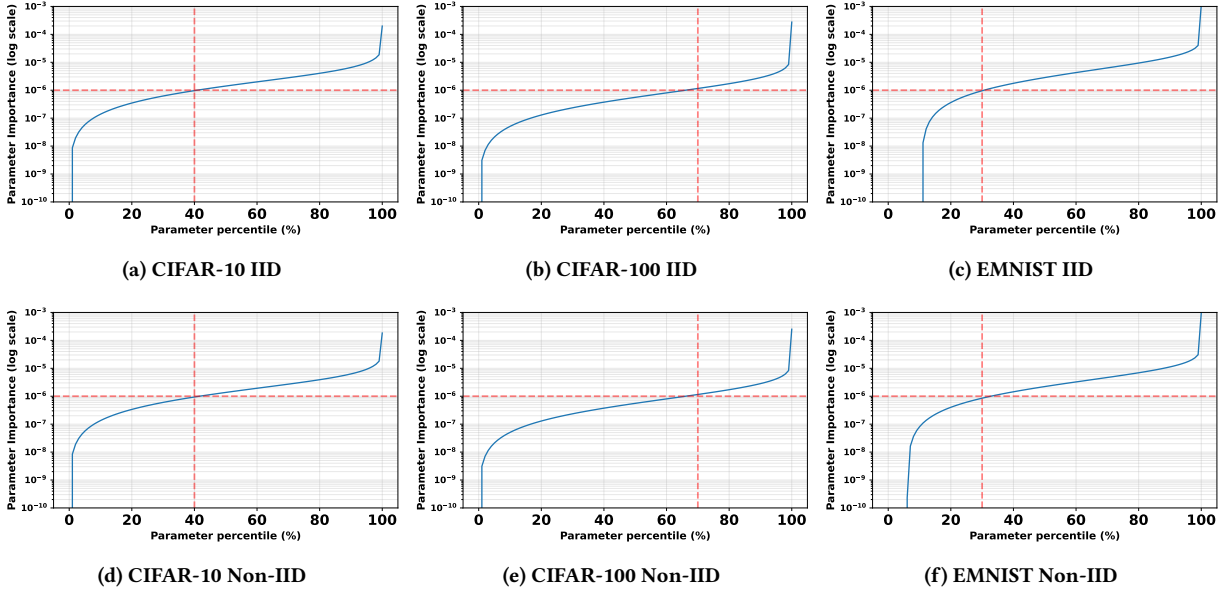


Figure H9: Parameter importance distribution.

unlearning dataset primarily depend on overlapping information. Therefore, in the context of unlearning, resetting redundant parameters is more effective and preferable to resetting important ones.

Appendix H.2 Pruning Ratio Selection

In Appendix F.1, we demonstrate how the pruning ratio ρ influences the unlearning performance. Therefore, in this section, we attempt to give a pruning ratio ρ selection rule.

As we discussed before, the optimal value of ρ depends on the distribution of memorization information across the model parameters. In other words, ρ depends the proportion of redundant parameters of D_r . This is because the non-overlapping information of D_u is irrelevant to the important parameters of D_r . Therefore, the main challenge lies in determining an appropriate threshold to identify important parameters of D_r . Subsequently, the pruning ratio ρ can be set based on the proportion of redundant parameters.

Actually, various indicators [8, 32] have been proposed to assess parameter importance for a given dataset on a neural network. For example, gradient-based input saliency maps [1] is a common tool. We apply this tool to analyze the parameter importance distribution on all unlearning tasks and provide the parameter importance distribution figures in Figure H9. Considering that the magnitudes of gradient updates often span multiple orders of magnitude, we apply the logarithmic function to visualize the distribution.

We measure the parameter importance distributions on CIFAR-10, CIFAR-100, and EMNIST under both IID and Non-IID conditions. Figure H9 illustrates similar trends across them. Most parameters exhibit extremely small importance (on the order of 10^{-8} to 10^{-6}), suggesting that they contribute minimally to the current optimization dynamics. As the percentile increases, parameter importance rises gradually and then sharply increases within the top few percent of parameters. This sharp rise typically begins around values

of 10^{-5} . This long-tailed distribution indicates that a small subset of parameters is very important, while the majority remain relatively inactive.

Based on this observation, we define parameters with importance values around or above the order of 10^{-5} as important. After that, we adaptively select the next lower order of magnitude, i.e., parameters with importance below the order of 10^{-6} , as redundant parameters. Using this adaptive method, the resulting pruning ratios for CIFAR-10 and EMNIST are approximately 0.3 to 0.4, while for CIFAR-100, the pruning ratio reaches around 0.7. These values are close to our empirical selections.

Additionally, when the task involves unlearning a larger number of clients, the pruning ratio should be increased, as the amount of relevant non-overlapping information grows. Data augmentation also requires a higher pruning ratio, since it promotes feature generalization and tends to enlarge redundant parameters. From the perspective of unlearning effectiveness, it is therefore often preferable to select a larger pruning ratio.

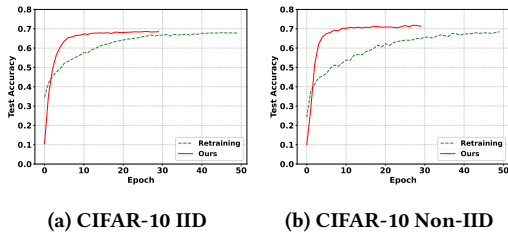
Appendix H.3 Extending to Class-level and Example-level Unlearning

Class-level Unlearning. Our approach can be easily applied to class-level unlearning without any modification. Moreover, class-level unlearning is generally easier than client-level unlearning since the overlapping information between different classes is minimal, which means we can apply a small pruning ratio $\rho = 0.2$.

We conduct class-level unlearning experiments with 10 clients on the CIFAR-10 dataset under both IID and Non-IID settings. The task involves unlearning all examples labeled as class 0 across all clients. Using FedMemPrune, the unlearning results are reported in Table H9, and a comparison of time consumption is presented in Figure H10.

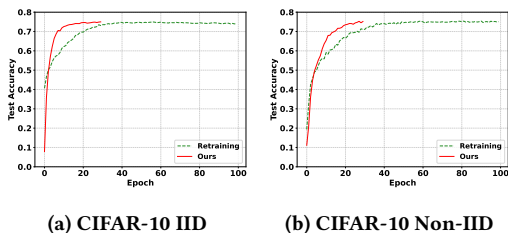
Table H9: Class-level task unlearning performance comparison.

	Unlearning Dataset Acc. (%)	Test Dataset Acc. (%)
CIFAR-10 IID		
Ours	0.00	68.45
Retrained Baseline	0.00	67.52
CIFAR-10 Non-IID		
Ours	0.00	71.32
Retrained Baseline	0.00	68.44

**Figure H10: Efficiency comparison for the class-level unlearning task.**

From the results, we observe that our method achieves complete unlearning performance on class 0 while maintaining strong generalization capability. Specifically, our method achieves unlearning accuracies of 0% under the two conditions. In terms of generalization performance, the test accuracies of 68.45% and 71.32% under IID and Non-IID settings, respectively, outperform the retrained baselines, which achieve 67.52% and 68.44% accuracy. Additionally, in terms of time efficiency, our method is 3× faster than the retrained baselines, demonstrating a significant advantage.

Example-level Unlearning. Regarding example-level unlearning, FedMemPrune can be directly applied. For efficiency, the system may accumulate multiple single-example unlearning requests and store them in a request stack. Once the stack reaches capacity or satisfies another predefined condition, the system executes the unlearning algorithm to remove the knowledge of these examples. Following the pipeline of FedMemPrune, we continue to reset redundant parameters with respect to the D_r and fine-tune on the D_r . Overall, in our approach, example-level unlearning is essentially similar to client-level unlearning.

**Figure H11: Efficiency comparison for the example-level unlearning task.**

We consider a scenario in which clients request the removal of 5,000 examples across 10 clients under both IID and non-IID settings using the CIFAR-10 dataset. Table H10 reports our results for this example-level unlearning scenario. Overall, the unlearning performance is comparable to client-level unlearning, achieving accuracy gaps of 5.33% and 1.00% on the most memorized subgroup. We also provide a time comparison in Figure H11, which illustrates the runtime difference between unlearning and full retraining. For both IID and non-IID cases, our approach consistently maintains a 50% improvement in efficiency.

Appendix H.4 Loss Surface of the Shortest Unlearning Path

In this section, we investigate the loss surface along the shortest path from the original model to any retrained model. Specifically, we compute the model difference vector and use it as a direction with a fixed step size to update the original model parameters. This simulates the unlearning process along the shortest path, allowing us to observe changes in the loss surface.

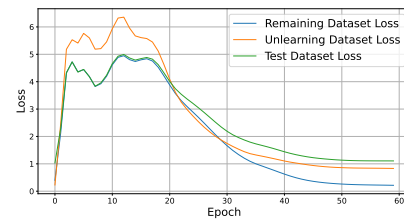
**Figure H12: Loss surface of the shortest unlearning path**

Figure H12 illustrates the loss surface during the unlearning process under CIFAR-10 Non-IID condition. Notably, the loss increases sharply when deviating from the original model parameters and gradually decreases as the model approaches the retrained state. This observation indicates that the original and retrained models lie in different loss basins. Furthermore, even slight perturbations to the original model can substantially degrade performance. In the context of unlearning, where specific knowledge must be removed from the model, this suggests a high risk of impairing generalization. After unlearning, the model must re-fit to the remaining data distribution.

From the perspective of the shortest path, unlearning can be interpreted as a partial re-training process, rather than simply reverting to a previous state of the original model. In cases involving substantial data removal, post-training or fine-tuning may be necessary to recover generalization performance. Moreover, our unlearning process exhibits behavior similar to that of the shortest path, and the observed transformation of the loss surface supports the validity of our unlearning algorithm.

Table H10: Example-level task unlearning performance comparison

	Accuracy by Unlearning Memorization Score Subgroup (%) ($\Delta \downarrow$)					Unlearning Dataset Acc. (%) ($\Delta \downarrow$)	Test Dataset Acc. (%) \uparrow	Local Fairness (10^{-3}) \downarrow
	Group (95%,100%]	Group (90%,95%]	Group (85%,90%]	Group (80%,85%]	Group (0%,80%]			
CIFAR-10 IID								
Ours	24.00 \pm 1.18 (5.33)	48.67 \pm 1.68 (5.20)	65.47 \pm 4.35 (1.34)	76.13 \pm 5.07 (8.14)	96.44 \pm 0.90 (2.38)	88.37 \pm 1.08 (1.28)	73.83 \pm 1.04	4.06 \pm 0.76
Retrained Baseline	18.67 \pm 0.75	43.47 \pm 0.50	64.13 \pm 0.19	84.27 \pm 0.19	98.82 \pm 0.07	89.65 \pm 0.06	73.84 \pm 0.30	0.11 \pm 0.03
CIFAR-10 Non-IID								
Ours	22.40 \pm 2.14 (1.00)	33.20 \pm 1.18 (4.00)	34.27 \pm 0.83 (2.81)	39.73 \pm 2.17 (3.20)	80.77 \pm 0.24 (0.29)	74.20 \pm 0.23 (0.37)	73.45 \pm 0.45	54.53 \pm 8.12
Retrained Baseline	21.40 \pm 0.20	29.20 \pm 0.57	31.46 \pm 0.50	42.93 \pm 1.86	81.06 \pm 0.62	74.57 \pm 0.27	74.89 \pm 0.14	25.86 \pm 15.54

This table shows the accuracies of the unlearned model Φ_{G_u} on the unlearning dataset D_u , its subgroups $\{T_p\}$ split by memorization scores and test dataset D_{test} , along with the local fairness metric under IID and Non-IID example-level unlearning.